



University of  
Stavanger

**Faculty of Science and Technology**

## **MASTER'S THESIS**

Study program/ Specialization: Structural and Material Science/Energy	Spring semester, 2010  Open / <del>Restricted access</del>
Author: Linn Garborg	(Author's signature)
Faculty supervisor: Professor Mohsen Assadi, University of Stavanger Supervisor(s): Nikolett Sipöcz, University of Stavanger	
Title of thesis: Physical Modeling of a Turbec T100 Microturbine	
Credits (ECTS): 30	
Key words: Gas turbine, microturbine, Turbec T100, heat and mass balance program, IPSEpro,	Pages: 73  + enclosure: 4  Stavanger, 15.06/2010 Date/year



## **Preface**

This master thesis has been written during the spring of 2010 at the department of structural and material science at the University of Stavanger, Norway.

I would like to acknowledge Professor Mohsen Assadi at the University of Stavanger for giving me the opportunity to work on this thesis. I also want to acknowledge Nikolett Sipöcz and Thomas Palmé, PhD students at the department, for coming up with the idea for this thesis. A special thanks to my supervisor, Nikolett Sipöcz, for helping me with IPSEpro. She has participated throughout the process and given me recommendations and guidance. Without her support it would have been difficult to carry out this master thesis.

I would also like to thank Kåre Bærheim, senior scientific officer, at the department for providing me with necessary weather data.

At Risavika Gas Centre I would like to acknowledge Øyvind Sundt, operations and HSEQ manager, for providing me with measurements utilized in this thesis.

## Abstract

The purpose for this thesis is to create a heat and mass balance model of the microturbine, Turbec T100, stationed at Risavika Gas Centre (RGC) in Tananger, Norway. The Turbec T100 at Risavika has some modifications due to research purposes. The combustion chamber is installed outside the casing of the Turbec and there is connected a bypass to it. These modifications also include additional sensors measuring pressure and temperature at the compressor outlet, after the recuperator and at the turbine inlet. The influence of the modifications on the performance of the Turbec is currently not known. By creating a heat and mass balance model the influence of the modifications, if any, can be discovered. With an accurate model of the Turbec T100 at RGC, it is possible to predict the performance data when running on other types of fuel than natural gas.

In order to create the model a literature study regarding the theory and thermodynamics of gas turbines has been carried out. As the Turbec T100 is a microturbine the literature study also involve the concept of microturbines and how they differ from regular gas turbines. A technical description of the Turbec T100 and the one stationed at RGC is also included.

The modeling of the Turbec T100 is done by the heat and mass balance program IPSEpro. A description of how to create a model of a gas turbine and how IPSEpro solves the implemented equations is described step-by-step. One of the tools within IPSEpro is called PSExcel. With this tool it is possible to do variations in a created model and get requested output data presented in an excel work sheet. In this thesis PSExcel has been used to generate data for Mats Mathisen's master thesis, *Noise Filtering from a Nonlinear System by Using AANN*.

To validate the model, measurements from RGC was implemented to the heat and mass balance model. IPSEpro calculated the power output and this was compared to the power output measured at Risavika. During the validation process it was revealed that the calculated power output did not correspond to the power output measured at Risavika. The calculated power output was very unstable and, surprisingly, the unit became power consuming instead of power producing. This indicated that there was some inaccuracy involving the measurements applied to the model.

# Table of Contents

Preface.....	iii
Abstract .....	iv
Table of Contents .....	v
List of Figures .....	vii
List of Tables.....	ix
Nomenclature .....	x
1 Introduction .....	1
1.1 Background.....	1
1.2 Objectives .....	1
1.3 Limitations.....	1
1.4 Methodology.....	2
1.5 Outline of the Thesis.....	2
2 Gas Turbine Introduction .....	4
2.1 Ideal and actual cycles .....	4
2.1.1 Isentropic Efficiency .....	5
2.1.2 Polytropic efficiency .....	7
2.1.3 Total efficiency .....	8
2.1.4 Ambient Conditions .....	9
2.2 Recuperating cycle .....	10
2.3 Compressor.....	13
2.3.1 Centrifugal compressor .....	13
2.3.2 Axial compressor.....	15
2.4 Combustion chamber .....	15
2.4.1 Combustor design.....	16
2.4.2 Methods for reducing emissions .....	17
2.4.3 Cooling systems .....	19
2.5 Turbine.....	20
2.5.1 Radial flow turbine.....	20
2.5.2 Axial flow turbine .....	21
3 Microturbine.....	24
3.1 Definition of a microturbine .....	24
3.2 Turbec T100 Microturbine .....	26
3.2.1 Main components .....	26
3.2.2 Auxiliary Systems .....	27

3.2.3	Turbec T100 at Risavika Gas Centre .....	27
4	Heat and Mass Balance Program .....	29
4.1	General.....	29
4.2	IPSEpro.....	30
4.2.1	Process Simulation Environment .....	30
4.2.2	PSExcel .....	40
4.2.3	Model Development Kit.....	43
4.2.4	Identification of HMB Equations Relevant for Validation Purposes.....	43
5	Modeling Turbec T100.....	45
6	Validation of the Turbec T100 Model.....	48
6.1	Composition of the Natural Gas .....	48
6.2	Ambient Condition Measurements .....	49
6.3	SCADA-system measurements .....	49
6.4	Turbec Internal Measurement System .....	49
6.5	AC-flow Measurements.....	50
6.6	Synchronization of the Measured Data .....	50
7	Results and Discussion.....	53
8	Conclusion and Future Work .....	60
	Bibliography.....	62
	Appendix .....	63

## List of Figures

Figure 2.1 A schematic gas turbine and the Brayton cycle	4
Figure 2.2 Efficiency of an ideal cycle	5
Figure 2.3 The actual cycle	6
Figure 2.4 Isentropic efficiency	8
Figure 2.5 Process scheme of a gas turbine with a recuperator	10
Figure 2.6 Comparing two turbines	11
Figure 2.7 Recuperating cycle	11
Figure 2.8 Efficiency, simple cycle with recuperator [2]	12
Figure 2.9 Surge- and chokepoint shown with a constant speed curve	13
Figure 2.10 Pressure and velocity through a centrifugal compressor [3]	14
Figure 2.11 Variation of enthalpy, velocity and pressure through an axial compressor [3]	15
Figure 2.12 Can-type combustor [4]	16
Figure 2.13 Cannular combustor [4]	17
Figure 2.14 Annular combustor [4]	17
Figure 2.15 Formation of CO, UHC and NO <sub>x</sub> as a function of temperature	18
Figure 2.16 Convection cooling [6]	22
Figure 2.17 Film cooling of a turbine blade [6]	22
Figure 2.18 Transpiration cooling [6]	23
Figure 3.1 Process scheme of the Turbec T100	27
Figure 3.2 Process scheme of the Turbec T100 at RGC [Nikolett Sipöcz]	28
Figure 3.3 Scheme of the Turbec T100 at RGC with measuring locations [11]	28
Figure 4.1 A screenshot of the PSE window	30
Figure 4.2 Settings of the compressor	31
Figure 4.3 Settings of the ambient conditions	31
Figure 4.4 Results presented in the flow sheet	32
Figure 4.5 Compressor and combustion chamber linked together	33
Figure 4.6 List of warnings	33
Figure 4.7 Compressor + combustion chamber	34
Figure 4.8 Model of a gas turbine cycle	35
Figure 4.9 Generator settings and output	36
Figure 4.10 The gas turbine with a recuperator installed	37

Figure 4.11 Number of iteration steps and accuracy	38
Figure 4.12 The gas turbine cycle is over defined	39
Figure 4.13 The gas turbine cycle is undefined	40
Figure 4.14 Scheme of data exchange between PSE and Excel [12]	40
Figure 4.15 Creating a variation in PSExcel	41
Figure 4.16 Selecting variation parameter	41
Figure 4.17 Results from the variation	42
Figure 4.18 Temperature and power output plotted in a graph	42
Figure 5.1 Process Scheme of Turbec T100	45
Figure 5.2 Modeled Turbec T100 containing a counter flow heat exchanger	46
Figure 6.1 Power output given by the internal system on the Turbec T100	51
Figure 6.2 Compressor outlet pressure given by the additional system	52
Figure 7.1 Power output	57
Figure 7.2 Electrical efficiency	59



## List of Tables

Table 4.1 HMB equations	44
Table 5.1 Assumptions implemented in the model	45
Table 5.2 Parameters of variation	47
Table 6.1 Composition of the natural gas	48
Table 6.2 Conversion of mol fractions to mass fractions	49
Table 6.3 Time periods for when the cooling valve was closed	50
Table 6.4 Frequency of the measurements	51
Table 7.1 Measurements from RGC inserted in the model	53
Table 7.2 Results from the calculation	54
Table 7.3 Measurements from RGC inserted in the model	55
Table 7.4 Results from the calculation	55
Table 7.5 Measurements from RGC inserted in the model	56
Table 7.6 Results from the calculation	57

# Nomenclature

## Notations

T	Temperature
S	Entropy
P	Static pressure
$P_0$	Stagnation pressure
$\eta$	Efficiency
$\eta_C$	Isentropic efficiency compressor
$\eta_T$	Isentropic efficiency turbine
eta_sturb	Isentropic efficiency turbine
$\eta_P$	Polytropic efficiency
$\pi$	Pressure ratio
w	Specific work
h	Enthalpy
Q	Heat
q	Specific heat
c	Specific heat capacity
v	Specific volume
R	Relative gas constant
m	Mass
$\varepsilon$	Effectiveness
$\rho$	Density
phi	Relative humidity

## Abbreviations

RGC	Risavika Gas Centre
AANN	Autoassociative neural network
UHC	Unburned hydrocarbons
TIT	Turbine inlet temperature
TIP	Turbine inlet pressure
TOT	Turbine outlet temperature
COT	Compressor outlet temperature

COP	Compressor outlet pressure
RH	Relative humidity
IGV	Inlet guide vanes
EPA	Environmental Protection Agency
SCR	Selective catalytic reduction
CHP	Combined heat and power
LPG	Liquefied petroleum gas
PMC	Power module controller
HE	Heat exchanger
HTX	Heat exchanger
HMBP	Heat and mass balance program
HMB	Heat and mass balance
PSE	Process simulation environment
MDK	Model development kit

# 1 Introduction

## 1.1 Background

The Turbec T100 installed at Risavika Gas Centre (RGC) in Tananger, Norway has some modifications due to research purposes. How these modifications affect the performance of the turbine is in present-day not known. By creating a model of the Turbec T100 in the heat and mass balance program, IPSEpro, and implementing measurements taken by RGC into the model, the performance parameters such as isentropic efficiencies, pressure ratio, pressure drops etc. of the Turbec could be discovered. By having an accurate model of the Turbec it is possible to predict, in advance, the power output and other performance measure of the system when it is running on other types of fuel than natural gas.

RGC provided four days of operational data for this project. This made it possible to make a validation of the simulated model of the Turbec T100.

## 1.2 Objectives

- Learn how to build models in IPSEpro and obtain an understanding how this software solves the implemented equations.
- Understanding the theory and the thermodynamics of gas turbines and implementing this knowledge to develop a model of the Turbec T100 in IPSEpro.
- Understanding the difference between a gas turbine and a microturbine, and how the Turbec T100 at RGC differs from a standard Turbec T100.
- Generate data for Mats Mathisen's master thesis *Noise Filtering from a Nonlinear System by Using AANN*, by utilizing the PSEExcel tool from IPSEpro.
- Validate the model of Turbec T100 by applying measurements from RGC into the model and comparing the calculated power output and the measured power output.

## 1.3 Limitations

- The modeling work is denoted to a specific microturbine from which the data are collected. No effort has been done to make the model applicable to other microturbine configurations

- The measurements applied to the model are only from the specific test period performed in April 2010 when the Turbec was operating on full load and the cooling air valve shut off.
- The components used to build up the model are used as they are i.e. with no modifications done by the MDK tool in IPSEpro.
- There has been no validation process of the water cycle connected to the Turbec at RGC.

## **1.4 Methodology**

In order to reach the stated objective the thesis was conducted by the following methodology:

- Learning IPSEpro by doing given exercises regarding modeling steam cycles, gas turbine cycles and combined cycles.
- A literature study regarding the concept of gas turbines, microturbines and heat and mass balance programs in general. This was completed in order to provide a theoretical foundation on which the modeling part is based.
- The model was made based on a process diagram of the Turbec T100.
- Implementing measured data from RGC into the model in order to validate it.

## **1.5 Outline of the Thesis**

- Chapter 1 Describes the background, objectives and limitations of the work, as well as the methodology that has been used.
- Chapter 2 Gives an introduction to the theory of gas turbines.
- Chapter 3 Describes the concept of microturbines and how they differ from regular gas turbines. A technical description of a regular Turbec T100 and the one stationed at RGC is also included.
- Chapter 4 Provides a brief introduction to heat and mass balance programs and a further description of how to model in PSE and how it solves the implemented equations. A short description of PSExcel and MDK is also included.

- Chapter 5 Describes how the Turbec T100 was modeled and which data was generated for further processing.
- Chapter 6 Describes the different measuring systems at RGC and how they were synchronized.
- Chapter 7 Provides a presentation of the results with a following discussion.
- Chapter 8 Presents a conclusion and a base for future work.

## 2 Gas Turbine Introduction

In this chapter the concept of a gas turbine will be described. At first the differences between the ideal and real cycles will be discussed. Then the main components in the gas turbine will be presented.

### 2.1 Ideal and actual cycles

A gas turbine utilizes the flow from hot gases produced from combustion of gas or fuel oil, to produce kinetic energy. When a generator is connected to the gas turbine, the kinetic energy is converted to electricity. The gas turbine consists of three main parts i.e. compressor, combustion chamber and turbine. Fresh air is drawn in to the compressor. As the air gets compressed, the pressure and temperature rises. The compressed air proceeds into the combustion chamber, where fuel is ignited. The high temperature exhaust gases enter the turbine, where they expand to atmospheric pressure while producing power.

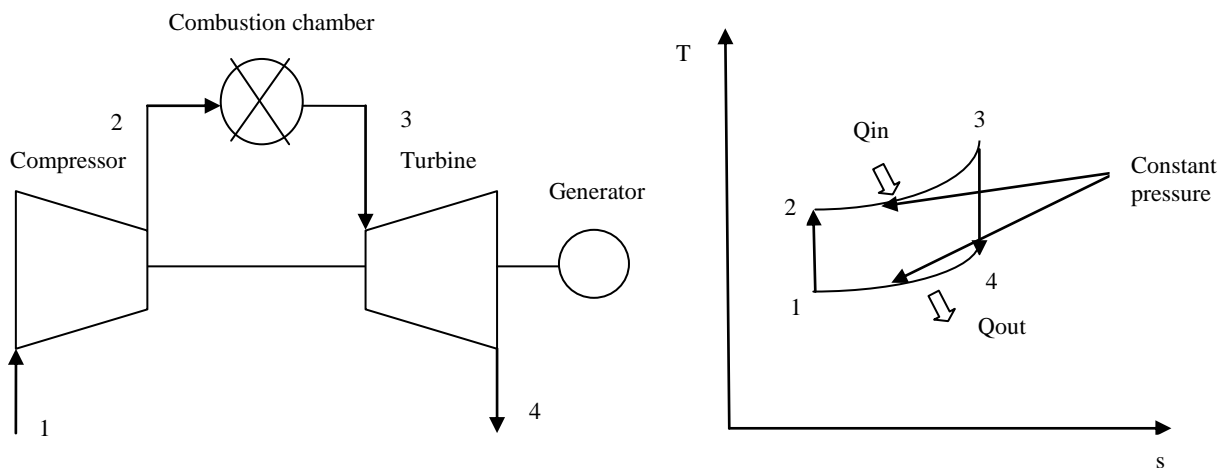
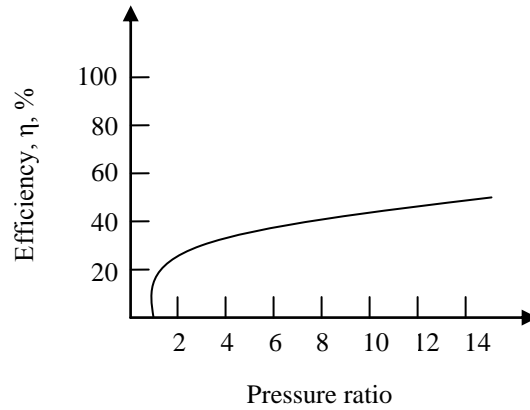


Figure 2.1 A schematic gas turbine and the Brayton cycle

The T-s-diagram in Figure 2.1 shows an ideal gas cycle, also known as the Brayton cycle. The Brayton cycle is made up of four internally reversible processes [1]:

- 1-2 Isentropic adiabatic compression
- 2-3 Combustion at constant pressure
- 3-4 Isentropic adiabatic expansion
- 4-1 Heat rejection at constant pressure

Turbomachines are essentially adiabatic i.e. no heat loss to the surroundings.



**Figure 2.2 Efficiency of an ideal cycle**

The efficiency of the gas turbine increases with the pressure ratio as shown in Figure 2.2.

Due to friction and turbulence an actual cycle is not reversible [2]. That means for the real cycle the compression and expansion is non-isentropic, and there are pressure losses throughout the cycle, this will reduce the total efficiency of the cycle with approximately 10 %.

### 2.1.1 Isentropic Efficiency

The isentropic efficiency is a measure of the deviation of actual processes from the corresponding idealized ones [1]. A compressor is a power consuming component. The actual required work for a compressor is therefore larger than the ideal work. The specific work can be expressed in terms of enthalpies,  $h$ . The isentropic efficiency for a compressor is defined by

$$\eta_c = \frac{\text{Isentropic compressor work}}{\text{Actual compressor work}} = \frac{w_s}{w_a} = \frac{h_{02'} - h_{01}}{h_{02} - h_{01}} \quad (2.1)$$

The turbine produces power, and the actual power output is less than the isentropic power output. The isentropic efficiency for a turbine is defined by

$$\eta_T = \frac{\text{Actual turbine work}}{\text{Isentropic turbine work}} = \frac{w_a}{w_s} = \frac{h_{03} - h_{04}}{h_{03} - h_{04'}} \quad (2.2)$$



Now taken the isentropic efficiency and the pressure losses into account, the T-s diagram for a gas turbine could look as illustrated in Figure 2.3.

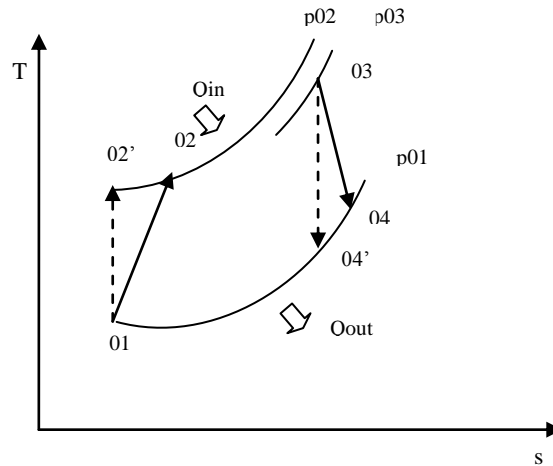


**Figure 2.3 The actual cycle**

01-02' Isentropic adiabatic compression

01-02 The compression taken the isentropic efficiency of the compressor into account

02-03 The combustion taken the pressure loss into account

03-04' Isentropic adiabatic expansion

03-04 The expansion taken the isentropic efficiency of the turbine into account

The equations above are not very useful in practice, because the isentropic states,  $h_{02'}$  and  $h_{04'}$ , do not correspond to any physical state in the turbomachine [5]. In order to make them more useful the enthalpies can be expressed by specific heat capacity and temperature.

$$\Delta h = c_p \cdot \Delta T \quad (2.3)$$

As the isentropic temperature is not known, the relation between pressures and temperatures can be used. This is because the isentropic pressure is equal to the actual pressure, as seen in Figure 2.3.

The relation between pressure and temperature can be expressed as

$$\frac{p}{T^{\kappa/\kappa-1}} = constant \quad (2.4)$$

Where  $\kappa$  is the relation between the specific heat capacities at constant pressure and constant volume,  $c_p$  and  $c_v$ , and the temperature is denoted in Kelvin.

The isentropic efficiencies for compressor and turbine can then be expressed as respectively

$$\eta_c = \frac{(p_{02}/p_{01})^{(\kappa-1)/\kappa} - 1}{(T_{02}/T_{01}) - 1}, \quad (2.5)$$

$$\eta_t = \frac{1 - (T_{04}/T_{03})}{1 - (p_{04}/p_{03})^{\kappa-1/\kappa}} \quad (2.6)$$

### 2.1.2 Polytropic efficiency

The isentropic efficiency considers only the start and end states of the compression and expansion processes. It does not take the actual paths of compression and expansion into account. This could be a disadvantage when analyzing a gas turbine containing several stages in the compressor or/and turbine. By performing a polytropic analysis during the compression and expansion the actual work can be determined more accurate than by an isentropic analysis. When working with a multistage machine, where the stages are identical and have the same stage pressure ratio and isentropic efficiency, the isentropic efficiency of the whole machine is not equal to that of a stage [5]. Calculating the work of a polytropic process summates the work of each stage.

The polytropic efficiency is defined by:

$$\eta_p = \frac{v dp}{c_p dT} \quad (2.7)$$

If the polytropic efficiency is constant for the whole process, the temperatures and pressure ratios of a stage can be related by making the substitution  $v = RT/p$ , where  $R$  is the relative gas constant.  $R$  divided by  $c_p$  is equal to  $(\kappa - 1)/\kappa$  and gives the differential equation

$$\frac{dT}{T} = \frac{\kappa - 1}{k\eta_p} \frac{dp}{p} \quad (2.8)$$

By integrating equation 2.8, the polytropic efficiency could be expressed as:

$$\frac{T_{02}}{T_{01}} = \left(\frac{p_{02}}{p_{01}}\right)^{(\kappa-1)/\kappa\eta_p} \quad (2.9)$$

When comparing equation 2.4 and 2.9 it occurs that there are algebraic relationships between the isentropic and polytropic efficiencies for the compressor and turbine:

$$\eta_c = \frac{(p_{02}/p_{01})^{(\kappa-1)/\kappa} - 1}{(p_{02}/p_{01})^{\kappa-1/\kappa\eta_p} - 1} \quad (2.10)$$

$$\eta_t = \frac{1 - (p_{04}/p_{03})^{(\kappa-1)/\kappa\eta_p}}{1 - (p_{04}/p_{03})^{\kappa-1/\kappa}} \quad (2.11)$$

By plotting equation 2.10 and 2.11 it is revealed that for a given polytropic efficiency the isentropic efficiency for a compressor decreases as the pressure ratio increases. At the same time the isentropic efficiency for a turbine increases when the pressure ratio increases [5].

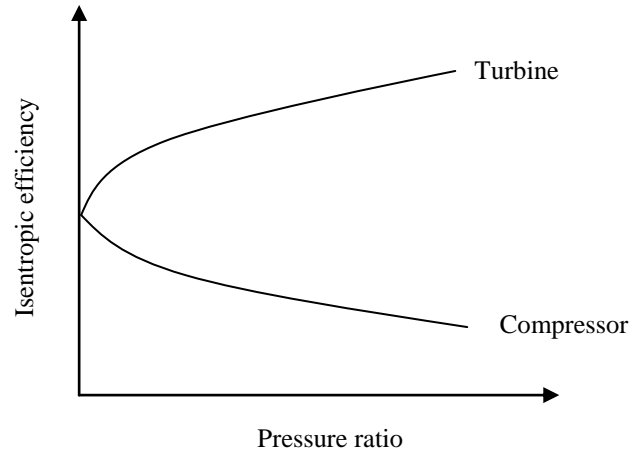


**Figure 2.4 Isentropic efficiency for a given polytropic efficiency**

### 2.1.3 Total efficiency

The total efficiency depends on the amount fuel injected and the power output. The compressor utilizes power from the turbine. The connection between compressor and turbine can be arranged in several ways. One is the single shaft arrangement (as illustrated in Figure

2.1), where the compressor, turbine and generator are operated on the same shaft. Another example is the twin shaft arrangement. In this arrangement there are two turbines; one high pressure turbine that drives the compressor and one low pressure turbine driving the generator. The most optimal arrangement depends on the operational conditions [2].

The efficiency of a gas turbine is given by

$$\eta_{total} = \frac{w_T - w_C}{q_{in}} \cdot \eta_{mech} \quad (2.12)$$

Where  $q_{in} = h_{03} - h_{02} = c_{p \text{ gas}} \cdot T_{03} - c_{p \text{ air}} \cdot T_{02}$

$$w_T = h_{03} - h_{04} = c_{p \text{ gas}} (T_{03} - T_{04})$$

$$w_C = h_{02} - h_{01} = c_{p \text{ air}} (T_{02} - T_{01})$$

These formulas are presented in the previous Figure 2.3.

The  $h$  is the enthalpy and  $c_p$  is the specific heat capacities for the air and exhaust gases.

$\eta_{mech}$  = the mechanical efficiency of the generator

As seen on the turbine work output a high inlet temperature gives greater efficiency. However, there is a limiting factor due to the ability in the material, used in the turbine blades and combustion chamber, to withstand the high temperature [2].

The total efficiency of a gas turbine is approximately between 30 – 45 % [3]. By using a heat exchanger, which utilizes the exhaust gas from the turbine outlet to preheat the air before combustion, the total efficiency could be improved. A description of recuperated gas turbines is described in more detail in section 2.2. Another alternative is the combined cycle, where the hot exhaust gas is used for boiling water to be expanded in steam turbines. With the last mentioned combination the total efficiency could reach 63 % [3].

#### 2.1.4 Ambient Conditions

When analyzing a thermal heat and power plant the reference state is often set to the surroundings, which is represented by the standard atmosphere. The standard atmosphere according to ISO 11086 has a pressure of 101,3 kPa, an air/cooling water temperature of 15 °C and a relative humidity of 60 % [9]. This is only the standard values and varies in the real world. As seen in the previous chapters the performance of a gas turbine depends on efficiency, pressure drop and heat loss. However, it also depends on the ambient conditions.

The air density depends on the pressure and temperature. Lower pressure reduces the density and hence reduces the mass flow rate and thereby reduces the power output. Increased ambient temperature has the same influence on the density as with the ambient pressure. This will result in a lower mass flow rate and the power output will be reduced. If the relative humidity increases, with the other conditions remaining constant, the power output will increase. This is because higher levels of humidity, there will be higher water content of the working medium of the gas cycle, resulting in a higher enthalpy drop in the gas turbine [10].

**2.2 Recuperating cycle**

Hot exhaust gases from the turbine could be utilized to preheat the compressed air entering the combustion chamber. A recuperator is then installed, and functions as a counter flow heat exchanger, as shown in Figure 2.5.

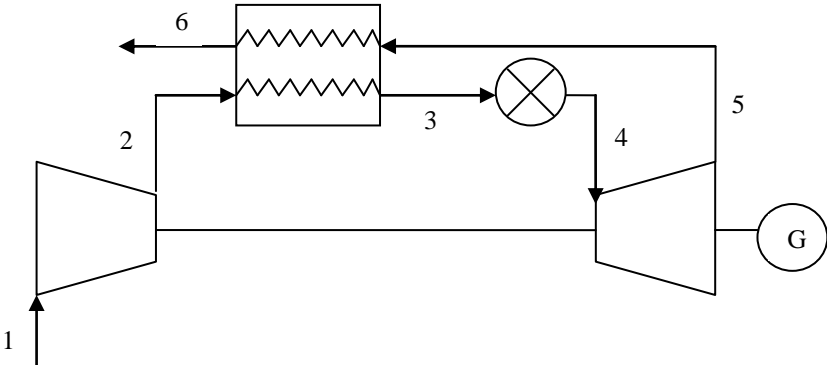


**Figure 2.5 Process scheme of a gas turbine with a recuperator**

By preheating the compressed air less heat needs to be produced in the combustion chamber, resulting in less fuel needed and hence the total efficiency is improved. It is important that the pressure ratio is not too high. As an example, by comparing two turbines, they have the same turbine inlet temperatures and different pressure ratios. The pressure of the exhaust gases leaving the turbines is equal. As seen in the T-s diagram in Figure 2.6 the turbine outlet temperature of the turbine operating with a higher pressure ratio is lower than the one with lower pressure ratio. And hence the turbine with the lower pressure ratio is more suitable for recuperating than the one with high pressure ratio. Thus most recuperators are used in small gas turbines such as microturbines, which are characterized by having low pressure ratios.

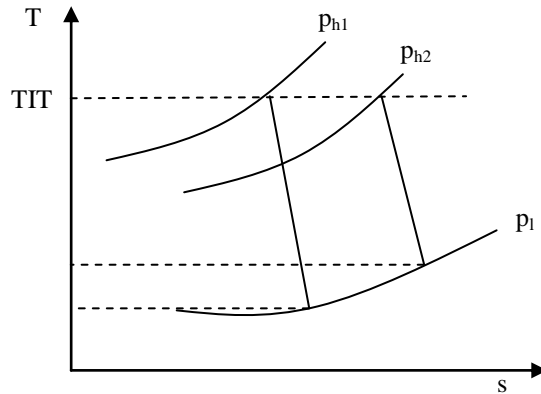


**Figure 2.6 Comparing two turbines**

The recuperated cycle is illustrated in the T-s diagram in Figure 2.7, it should be noted that it does not take the pressure losses through the recuperator or the combustion chamber into account. As seen in Figure 2.7 heat from the exhaust gases,  $Q_R$ , is used to preheat the compressed air between point 2-3.

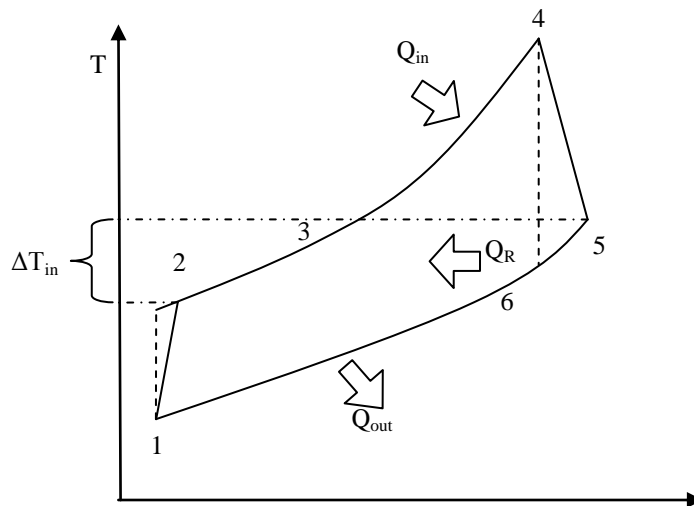


**Figure 2.7 Recuperating cycle**

For an ideal recuperating cycle the exhaust temperature is equal to the temperature of air leaving the recuperator i.e.  $T_3$  is equal to  $T_5$  in Figure 2.7. Due to heat losses to the surroundings this does not happen in reality. Assuming the recuperator to be well insulated

and any changes in the kinetic and potential energies to be negligible the maximum heat transfers from the exhaust gases to the air can be expressed as [1]:

$$q_{ideal} = h_5 - h_2 = (c_{p\ gas} \cdot T_5) - (c_{p\ air} \cdot T_2) \quad (2.13)$$

and

$$q_{actual} = h_3 - h_2 = c_{p\ air}(T_3 - T_2) \quad (2.14)$$

From these equations the effectiveness i.e. how close the recuperator is to an ideal recuperator can be calculated. The effectiveness  $\varepsilon$  is defined as

$$\varepsilon = \frac{q_{actual}}{q_{ideal}} \quad (2.15)$$

Based on Figure 2.7, the total efficiency of the cycle can be expressed as:

$$\eta_{tot} = \frac{c_{p\ gas}(T_4 - T_5) - c_{p\ air}(T_2 - T_1)}{(c_{p\ gas} \cdot T_4) - (c_{p\ air} \cdot T_3)} \quad (2.16)$$

As shown in Figure 2.8, the efficiency of the recuperating cycle decreases when the pressure ratio increases. The stippled line symbolizes the efficiency of the simple cycle (as in Figure 2.2) and  $t$  is the temperature ratio between  $T_4$  and  $T_1$ . When  $T_2$  is larger or equal to  $T_5$  the efficiency lines intersect and the recuperator is no longer useful.

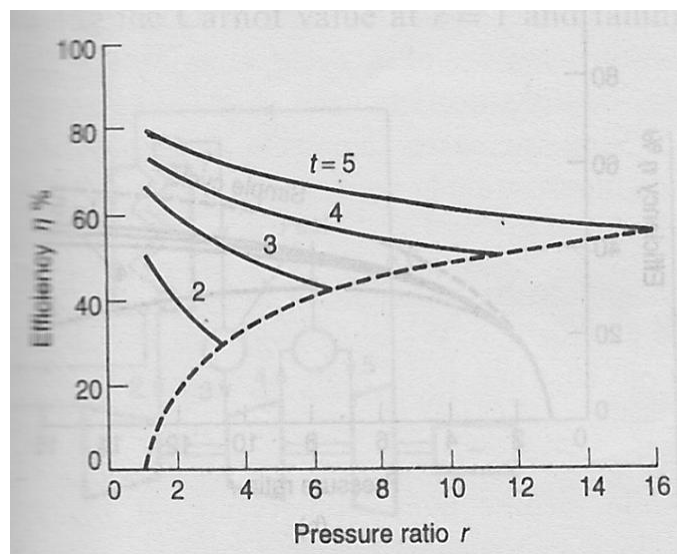


Figure 2.8 Efficiency, simple cycle with recuperator [2]

## 2.3 Compressor

In this chapter both centrifugal and axial compressors will be described.

A pressure ratio must be provided in order to produce an expansion through a turbine. The compression of air is therefore a necessary step in the system. As air is a compressible medium, the compressor increases the pressure by reducing the volume of the gas.

The operating range for a compressor is between the surge point and the choke point, as shown Figure 2.9. The surge and choke point depends on the pressure ratio in the compressor and the flow rate.

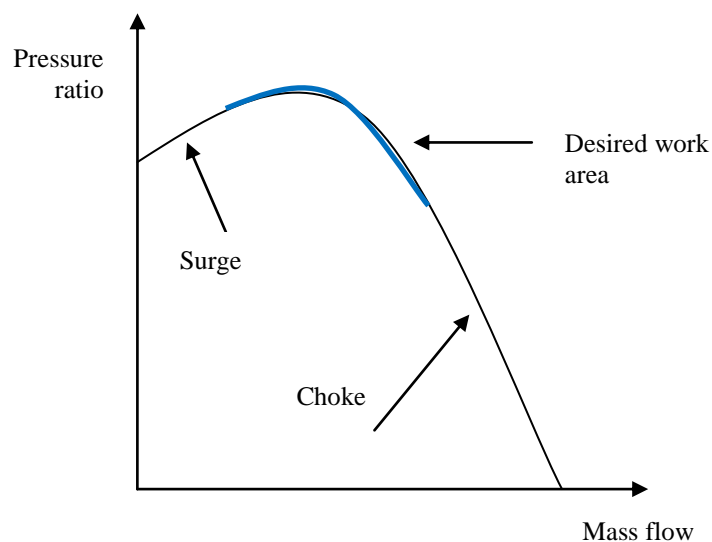


**Figure 2.9 Surge- and chokepoint shown with a constant speed curve**

If the flow rate reduces, it leads to a loss of delivery pressure, and the flow will be reversed. This is called surge. Choking occurs when the flow increases to the relative speed of sound. The impeller vanes are not designed to handle this amount of flow, and will cause a loss in delivery pressure. Surge is something that needs to be avoided; mainly because of the forces acting on the compressor when the flow is reversed, may lead to a total destruction. Choke conditions cause a large decrease of the efficiency, but do not lead to destruction of the unit [3].

### 2.3.1 Centrifugal compressor

A centrifugal compressor consists of a stationary casing containing inlet guide vanes, an inducer, a rotating impeller, a number of fixed diffusers and a scroll. The air comes into the



compressor through an intake duct and is given a prewhirl by the inlet guide vanes. The air is then sucked into the impeller eye and consisting an inducer where the direction is changed from axial to radial [3]. It is the centrifugal effect causing the air to flow radially outwards along the vanes to the impeller tip [4]. Because of the rotating impeller the air is accelerated and the static pressure increases between the impeller eye and the impeller tip. As the air flow through the diffuser, which is a divergent nozzle, the kinetic energy (velocity) is converted to pressure energy, as seen in Figure 2.10. The compressed air enters the scroll and is discharged.

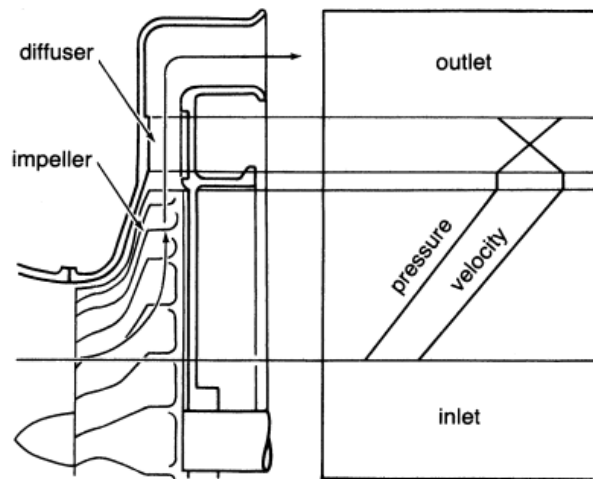


**Figure 2.10 Pressure and velocity through a centrifugal compressor [3]**

There will be a small pressure loss due to the friction in the diffuser [2]. The normal practice is to design the compressor so that about half of the pressure rise occurs in the impeller and the rest in the diffuser [4].

The pressure ratio in a centrifugal compressor varies between 3: 1 and 7: 1. This is a relatively small pressure ratio compared to axial compressors which can obtain an overall pressure ratio of 40: 1. Axial compressors need several compressor stages achieving the high pressure ratio, because one stage of the axial compressor only has a pressure ratio between 1,1: 1 and 1,4: 1. The centrifugal compressors on the other hand, increase the pressure in one stage. Because of this the centrifugal compressor takes less space than the axial compressor, and is a preferable choice in small gas turbines e.g. microturbines.

### 2.3.2 Axial compressor

An axial compressor is usually designed with multiple stages to fulfill required delivery pressure [2]. One stage consists of one rotor and one stator. The air is accelerated by a row of rotating blades and then decelerated by a row of stationary blades. The increase stagnation pressure i.e. the total pressure is accomplished by the rotor. As the air is accelerated in the rotor creating a dynamic pressure, the stator transforms this kinetic energy into an increase of static pressure, by decelerating the air flow as shown in Figure 2.11. The changes in the total conditions for pressure, temperature and enthalpy only occur in the rotating component i.e. the rotor, where the energy is supplied to the system.

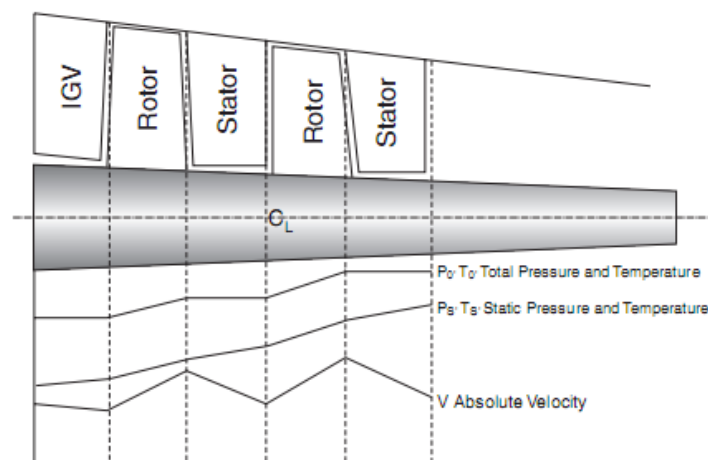


Figure 2.11 Variation of enthalpy, velocity and pressure through an axial compressor [3]

Due to friction there will be a loss in stagnation pressure between the rotor and stator [2].

As seen in Figure 2.11 the length of the blades and the annulus area is decreasing through the length of the compressor. The reason for this is to obtain a constant axial velocity, as the reduction of flow area compensate for the increase of density of the air as it is compressed [3].

As the axial compressor can have an overall pressure ratio of 40: 1, it dominates the field for industries needing large power [2].

### 2.4 Combustion chamber

In the combustion chamber the heated air is mixed with fuel e.g. natural gas or liquid petroleum distillates. At start up of the gas turbine the mix of fuel and air needs to be ignited by electric spark to initiate the combustion process. Thereafter the flame must be self-sustaining [2].

### 2.4.1 Combustor design

The design of the combustion chamber depends on whether the gas turbine is on an aircraft or on a ground-based system.

The can-type combustor consists of a number of separate chambers spaced around the shaft connecting the compressor and turbine, as shown in Figure 2.12. The air from the compressor is split into separate streams, each supplying a separate chamber. This arrangement is suitable for engines containing centrifugal compressors where the flow is divided into separate streams in the diffuser [2]. The advantage of can-type combustors is that they are easy to test and maintain, because it can be done on one single can rather than the whole combustion system. Can-type combustors were widely used on early gas turbines. Due to their high weight and relative large pressure drop, most modern gas turbines do not use can combustors today.

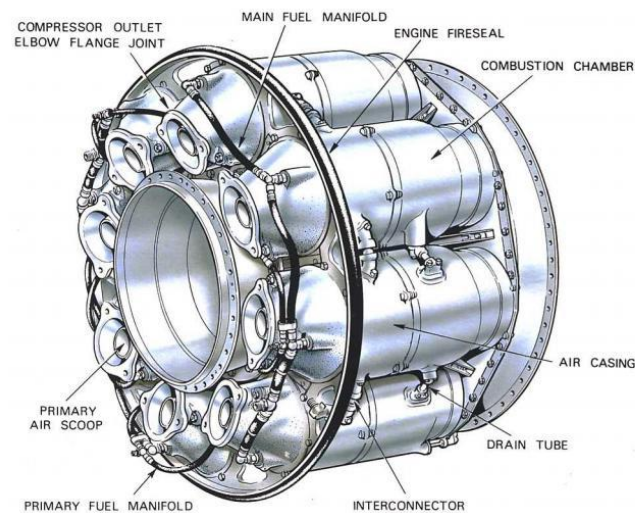


**Figure 2.12 Can-type combustor [4]**

Recent designs make use of cannular combustion chambers. As with the can-type combustor the cannular design also have separate combustion cans. It has individual flame tubes spaced around an annular casing [2], as illustrated in figure 2.13. Because of the annulus casing each can does not have to serve as a single pressure vessel, which results in a smaller pressure drop than the can-type design. The cannular combustion chamber is the preferred combustor type in most gas turbines. The reason for this is the relative low pressure drop, good temperature distribution and they are easy to maintain.

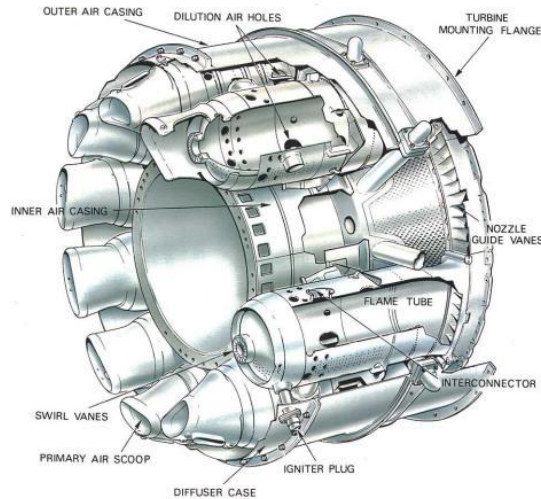


**Figure 2.13 Cannular combustor [4]**

The most compact combustion design is the annular combustor. This type of combustion consists of a single flame tube, which is contained in an inner and outer casing [4], as shown in Figure 2.14. Because of the compact design the combustor requires less space and saves a considerable amount of weight. A major advantage of the annular design is the wall area surrounding the system is much less than the systems described above, this results in less amount of cooling air and a higher turbine inlet temperature. Because of its low weight and low frontal area it is a preferred choice in aircraft engines.

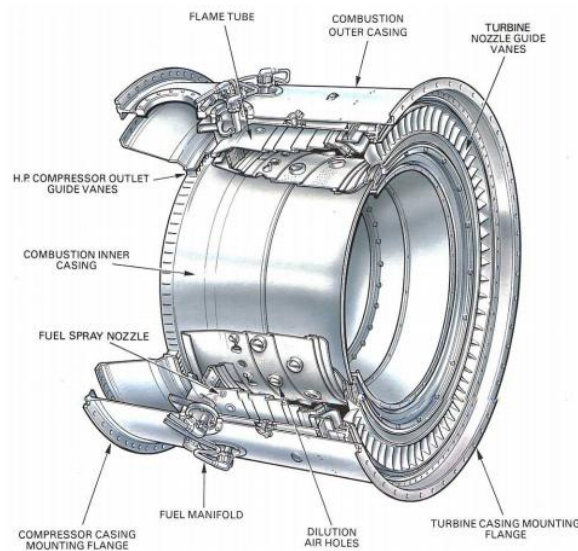


**Figure 2.14 Annular combustor [4]**

## 2.4.2 Methods for reducing emissions

When burning fuel it is desirable to achieve complete combustion to prevent dissociation of carbon monoxide (CO) and unburned hydrocarbons (UHC). CO is a very toxic pollutant that

must be controlled to very low levels. The amount of CO and UHC produced is increased if the flame temperature is low. NO<sub>x</sub> on the other hand is produced when the combustion temperature is high as illustrated in Figure 2.15. However, if the residence time of the fluid in the combustor is increased the formation of UHC and CO will be decreased, due to achievement of complete combustion. Increasing the residence time implies an increase in combustor cross-sectional area or volume [2].

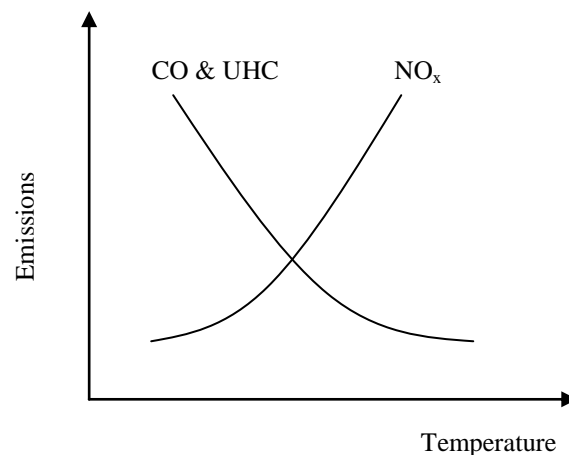


**Figure 2.15 Formation of CO, UHC and NO<sub>x</sub> as a function of temperature**

Due to high combustion temperature NO<sub>x</sub> is produced. In recent years the legislations of NO<sub>x</sub> emissions has been stricter, and has led to significant changes in the combustor design. The standard level of NO<sub>x</sub> set by Environmental Protection Agency (EPA) is 75 ppmvd (parts per million by volume of dry exhaust gas). Basically there are three major methods of minimizing emissions: water or steam injection into the combustor, selective catalytic reduction and dry low NO<sub>x</sub> [2].

The purpose of water/steam injection is to reduce the flame temperature. It is important that the water is de-mineralized to prevent corrosive deposits in the turbine. In the first installations there was injected half as much water as fuel. This resulted in a 40 % reduction in NO<sub>x</sub>. The amounts of water required today are substantial. Thus this type of installation is not a preferable choice in locations where water recourses are scarce and expensive. Also in locations where the ambient temperature is below freezing point there must be used other types of installations to reduce the NO<sub>x</sub> emissions. The power output will have a small increase as a result of a higher mass flow through the turbine, but there will be a decrease in thermal efficiency, because the TIT will be lowered. It has also been discovered that while continuing to decrease NO<sub>x</sub>, there will be an increase in both CO and UHC. The reason for this is when the flame temperature is decreased there will be an increase of CO and UHC as

illustrated in Figure 2.15. Steam injection operates at the same principle as water injection and is applied in systems producing steam e.g. cogeneration plant and combined cycles [2].

Selective catalytic reduction (SCR) has been used in applications where the specified limits of  $\text{NO}_x$  are extremely low. This unit is installed after the turbine cleaning up the exhaust gases. A catalyst is used together with injection of controlled amounts of ammonia ( $\text{NH}_3$ ) and results in a conversion of  $\text{NO}_x$  to  $\text{N}_2$  and  $\text{H}_2\text{O}$ . This conversion can only occur in a limited temperature range (285 – 400 °C) and the system is installed in the heat recovery steam generator. Thus it can only be used in applications containing a waste heat recovery system i.e. combined cycle systems. The difficulties with SCR are controlling the  $\text{NH}_3$  when dealing with variable loads and the handling and storage of the noxious fluid. The cost of using SCR system needs also to be taken into account [2].

The term dry low  $\text{NO}_x$  derives from the fact that there is no water involved when reducing the  $\text{NO}_x$  emissions. With this design the air and most of the fuel is premixed before entering the combustion chamber. The fuel/air ratio is then lean which reduces the flame temperature and hence the  $\text{NO}_x$  emissions are decreased [2]. The injector in the dry low  $\text{NO}_x$  technology has two fuel circuits, one (approximately 97 %) premixing the fuel with air and one injecting the rest of the fuel directly into the combustion chamber. The reason for this is when the gas turbine operates on part load the mixture of fuel/air can be too lean to burn, and a flame out can occur. A small portion of the fuel is burned richer in order to have a stable flame. A swirler is used to create the required flow conditions in the combustion chamber to stabilize the flame [3].

### **2.4.3 Cooling systems**

The combustor outlet temperature can be as high as 1850 K [2], this sets some requirements to the materials and cooling. The liner is the inner part of the casing which is exposed to the high temperatures radiated from the flame and combustion. To improve the life of the liner, it is necessary to lower the temperature of the liner and use a material that is resistant to thermal stress and fatigue. The air film cooling method reduces the temperature of the surface both inside and outside the liner. A metal ring is fastened inside the liner making an annular clearance. Some of the compressed air is used as coolant between the surfaces of the liner. In systems containing a combined cycle steam could be used as coolant instead of air.

The material of the liner being used is Nimonic 75, which is an 80-20 nickel-chromium alloy stiffened with a small amount of titanium carbide. This material has an excellent oxidation and corrosion resistance at elevated temperatures, a good resistance against fatigue and

reasonable creep strength. As the firing temperature has increased in the newer gas-turbine models, HA-188 has been employed. HA-188 is a chromium-nickel alloy which has improved the creep rupture strength. Many of today's combustors also have thermal barrier coatings. This is an insulation layer with a total thickness of 0,4- 0,6 mm and can reduce the metal temperature by 50- 150 °C [3].

## **2.5 Turbine**

After the compression and combustion the hot working exhaust gases expands through the turbine and produces power. As with the compressor there are two basic types of turbines; radial flow and axial flow. In this chapter both types will be described.

### **2.5.1 Radial flow turbine**

Basically the radial flow turbine is a centrifugal compressor with reversed flow and opposite rotation [3]. The gas flows with a high tangential velocity directed inwards, and leaves the rotor with as small whirl velocity as possible near the axis of rotation [2]. The appearance of the radial flow turbine is very similar to the centrifugal compressor, but instead of diffuser vanes, the radial flow turbine has a ring of nozzle vanes [2]. The nozzles transform the dynamic pressure into kinetic energy. To increase the efficiency of the turbine, the turbine outlet is connected to a diffuser [3]. The outlet diffuser converts the high absolute velocity into static pressure.

The work produced by a single stage radial turbine is equivalent to the work produced by two or more stages in the axial turbine. This phenomenon occurs because a radial flow turbine usually has a higher tip speed than an axial flow turbine. As the power output is a function of the square of the tip speed, the power produced by a radial flow turbine is greater than a single stage axial turbine [3].

In compact designs the gas turbine often consists of a centrifugal compressor mounted back-to-back with a radial flow turbine. The rotor then becomes short and rigid and hence more efficient. Radial flow turbines have also been widely used as a turboexpander in the cryogenic industry and in turbochargers for reciprocating engines [2]. In these systems the mass flow rate and pressure ratio is low. The radial flow turbine handles low flow rates more efficiently than axial flow.

In order for radial turbines to be cost effective they are installed without cooling system. A cooling system on this type of turbine would have to be very complex, due to the turbine wheel. This sets some limitations to the turbine inlet temperatures and material being used in

order for the turbine to sustain. Nickel alloys such as Inconel is often being used as turbine material. These materials can handle TITs up to 1000 °C.

Because of the cheap, compact and robust design, the radial flow turbine is a preferable choice in microturbines.

## **2.5.2 Axial flow turbine**

The vast majority of gas turbines employ the axial flow turbine. This is because the axial turbine is most efficient in most operational ranges [3].

The axial flow turbine can consist of one or more stages. As with the axial compressor, one stage of the axial flow turbine consists of one stator and one rotor. The stator consists of a row of nozzle blades, which decrease the pressure and temperature and increases the velocity. The kinetic energy from the stator is converted to mechanical energy through the rotor blades.

There are two types of axial flow turbines: The impulse type and the reaction type. In the impulse type turbine the entire enthalpy drops in the nozzle. This causes the flow to have a high velocity entering the rotor. The reaction turbine divides the enthalpy drop in the nozzle and the rotor. The impulse stage produces twice the output of a comparable 50 % reaction stage, but the efficiency is less than that of a 50 % reaction stage. The cost of a reaction turbine for the same amount of work as an impulse turbine is much higher this is because the reaction turbine requires more stages. A multistage axial turbine usually consists of impulse type turbines in the first few stages and reaction type turbines in the later stages. Building the turbine this way, the pressure drop in the first stages is maximized and a good efficiency is obtained [3].

### **2.5.2.1 Turbine blade cooling**

As axial turbines are used in large power plants that can produce hundreds of MW, they operate with high turbine inlet temperatures (TIT). Referring to equation 2.12 in chapter 2.1.3 it is desirable to have as high TIT as possible. The challenge for engineers today is to find materials and turbine blade cooling techniques that can handle these high temperatures. TIT could be higher than 1400 °C and the turbine blade alloys can only handle a temperature at approximately 870 °C. Advanced air cooling is needed to prevent destruction of the turbine components. There are five basic air-cooling schemes: Convection cooling, impingement cooling, film cooling, transpiration cooling and water/steam cooling [3].

Convection cooling was the most common cooling method in present-day gas turbines. With this design cooling is achieved by bleeding air from the compressor. The cooling air flows



inside the turbine blade or vane and removes the heat through the walls [3], as illustrated in Figure 2.16.

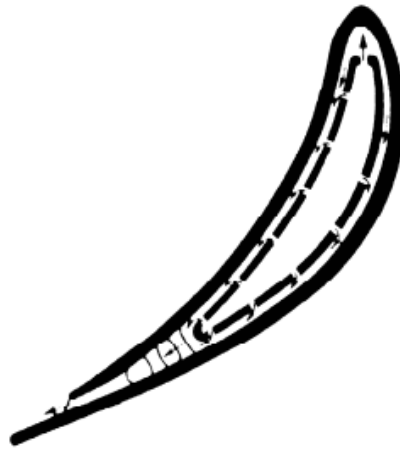


**Figure 2.16 Convection cooling [6]**

Impingement cooling is a high intensity form of convection cooling. The cooling air is blasted on the inner surface of the airfoil by high-velocity air jets. This permits an increased amount of heat to be transferred to the cooling air from the metal surface. As the temperatures can vary on the airfoil, the cooling air can be restricted to specific sections on the airfoil achieving even temperatures over the entire surface [3].

Film cooling allows the cooling air to form an insulating layer between the walls of the blade and the hot gas stream as illustrated in Figure 2.17. This way of cooling protects the airfoil the same way combustor liners are protected [3], as mentioned in chapter 2.4.3.

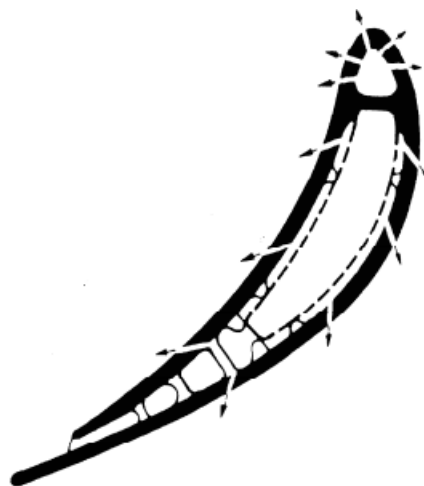


**Figure 2.17 Film cooling of a turbine blade [6]**

There is a porous shell surrounding the turbine blade. Transpiration cooling allows the cooling air to flow through the porous wall and cover the entire blade with coolant flow, as illustrated in Figure 2.18. The heat transfer is directly between the cooling air and the hot gases [3].

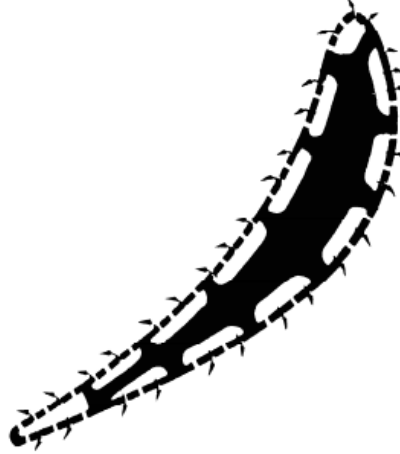


**Figure 2.18 Transpiration cooling [6]**

In water cooling designs there are a number of tubes inside the turbine blades to provide channels for the water. Due to good heat transfer conditions, the tubes are constructed from copper. By the time the water reaches the turbine blade tip it has converted to steam, thereby lower the turbine blade temperature, before it is injected into the flow stream i.e. the hot gases. This type of cooling system is currently in the experimental stage. If the gas turbine is connected to a steam cycle, i.e. a combined cycle the steam from the high pressure steam turbine can be used as coolant in copper tubes within the turbine blades [3].

## 3 Microturbine

In this chapter the definition of a microturbine will be presented. There will also be a description of the main components and auxiliary systems of the Turbec T100 microturbine. Due to some modifications on the Turbec T100 installed at Risavika Gas Centre the differences between this machine and a regular T100 are also discussed.

### 3.1 Definition of a microturbine

Microturbines are gas turbines that produce power approximately from 10 – 200 kW. Regular gas turbines however are marketed as 40 – 50 MW engines [8]. The intention with microturbines is to be a simple, flexible and low cost system. Achieving these characteristics would make microturbines excellent candidates for providing base load and cogeneration power for a range of commercial customers [3]. Microturbines usually come as a combined heat and power (CHP) system. The unit produces electricity as described in chapter 2.1 and utilizes the exhaust heat from the turbine to heat up water. This heated water could either be produced as steam to be expanded in a steam turbine or it could be used as district heating. By utilizing the waste heat the system achieves a higher total efficiency than systems that only produce electricity.

A regular microturbine consists of the following parts [8]:

- Radial compressor and turbine mounted back-to-back on a single shaft
- Combustor
- Recuperator and potentially a heat recovery unit
- High speed generator and a power conditioning system
- Casing and balance of plant

For systems producing up to 100 kW, radial turbo machinery is the most efficient [8]. Radial systems operate with a lower pressure ratio than axial systems. Due to the relative small power output a lower pressure ratio is needed. The rotating equipments i.e. the compressor and turbine is incorporated on a single shaft. This shaft is supported by bearings that are oil lubricated or air bearings [8].

Aluminum, titanium or Inconel are often used as materials for the compressor wheel. The turbine operates at much higher temperatures (up to 1000 °C) and this sets more requirements

to the material being used. Usually the turbine wheel is made of nickel alloys, such as Inconel [8].

A single can combustor is often used as combustion system in the microturbine, but some systems are installed with an annular combustor. The compressed air from the compressor is preheated by a recuperator before entering the combustion chamber.

As with all engines, utilizing hydro carbons or diesel as fuel, the microturbines produce  $\text{NO}_x$ . In order to reduce the  $\text{NO}_x$  emissions the microturbine is usually installed with the dry low  $\text{NO}_x$  system, where the fuel is premixed with air before it is ignited, as described in chapter 2.4.2. This results in a production of  $\text{NO}_x$  to be approximately 25 ppm (part per million) [8].

One major advantage of the microturbine to other heat engines is their capability to burn a variety of fuels. It can burn regular fuels such as natural gas, LPG and diesel, but it can also utilize waste and biomass as long as the calorific value is higher than  $4 \text{ kWh/Nm}^3$ .

If the microturbine was installed without a recuperator, the efficiency would be as low as 10 %, and even lower if it is operating on part load. This is due to the small size of the turbo machinery components which make the clearances analogically larger and thereby increasing the losses in the system. In larger units the pressure ratio is much higher, more expensive materials and cooling techniques allowing higher TITs making the clearances almost negligible. To cope with the problem regarding the losses in the microturbine, a recuperator is installed. The recuperator exchanges heat from the hot exhaust gases leaving the turbine with the compressed air. The air is now preheated, needing less heat i.e. fuel to achieve desired turbine inlet temperature, which increases the electrical efficiency of the system. Due to relative high temperatures the recuperator is often made of high grade stainless steel [8].

The turbo machinery in the microturbine rotates with a higher speed than a regular generator, thus a high speed generator is installed. This type of generator can rotate with 120 000 RPM and has an efficiency between 95 – 98 %. By using a high speed generator there is no need for a reduction gearbox. The generator works as a starting motor of the gas turbine. The generated electric power needs to be rectified and transformed to preferred frequency before entering the grid [8].

There is often built a casing around the microturbine to meet various electrical, noise attenuation and safety standards. Balance of plant (BoP) items usually includes filters, sensors, instrumentation, controls and wiring [8].

Microturbines are often used in systems requiring more power than piston engines and less power than regular gas turbines. There is a need for an economic analysis deciding whether several piston engines or a few microturbines are most cost efficient. Piston engines are very large units that require much space per unit power produced. Microturbines, on the other hand, have a small footprint and are a preferable choice where the space is limited. The amount of emissions and the cost of reducing these is one last factor needed to be taken into account when deciding which machinery to be chosen. Microturbines are often used as an emergency unit in places where the power supply is unsteady or in places where CHP is needed.

## **3.2 Turbec T100 Microturbine**

### **3.2.1 Main components**

The main components of the unit include a gas turbine engine, electrical generator, electrical system, exhaust gas heat exchanger and supervision- and control system. The gas turbine engine operates on a single shaft i.e. the compressor is mounted on the same shaft as the turbine and generator, as shown in Figure 3.1. Ambient air is drawn in to the unit and compressed by a centrifugal compressor. The pressure ratio for this system is about 4,5: 1. Compressed air leaving the compressor enters the recuperator, as illustrated in Figure 3.1. Preheated compressed air is mixed with natural gas and ignited and the combustion gases enter the turbine with a temperature at approximately 950 °C. The combustion gases expand through the turbine and leaves with a pressure close to atmospheric pressure and a temperature of approximately 650 °C. A permanent rotating magnet in the generator generates the electric power. The generated electric power needs to be rectified and transformed to preferred frequency before entering the grid [7].

After the expansion in the turbine the exhaust gases enter the recuperator before entering the gas-water counter-current heat exchanger with a temperature of approximately 270 °C. By regulating the mass flow of the water, the water is heated up to a desired temperature.

An automatic control system, PMC (Power Module Controller), supervises and controls the Turbec T100. This causes the system to shut down automatically in case of critical distortion. The PMC uses sensors to control heat demand, gas pressure, oil temperature and vibrations. If a critical condition occurs the PMC will shut down the system by either a normal stop or an emergency stop. Faults are displayed on the control panel and then logged in the system [7].

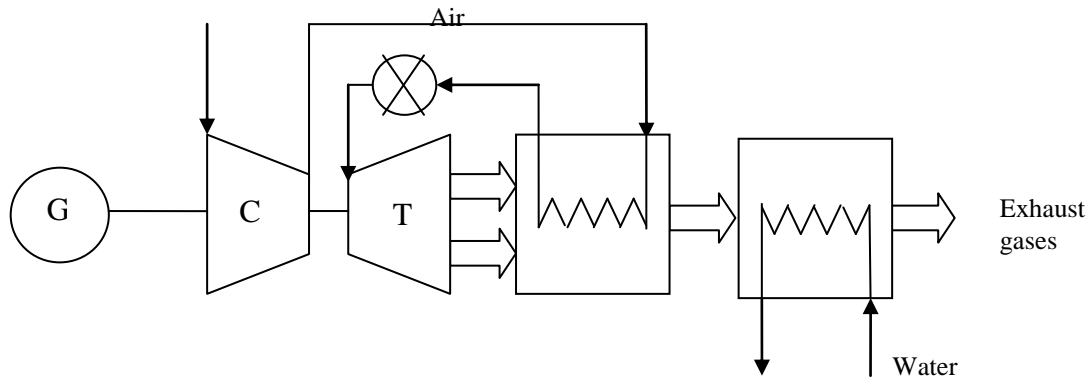


**Figure 3.1** Process scheme of the Turbec T100

### 3.2.2 Auxiliary Systems

Auxiliary systems include air intake, ventilation system, lubrication system, buffer air system, cooling system, fuel gas system and a fuel gas compressor. The air intake system consists of a filter to prevent foreign components to enter the cycle causing damages to the various components in the system. A ventilation system is needed to cool excess heat from the system. Lubrication is required for the rotating parts. Lubricating oil circulates through the bearings gaining heat from the system and is cooled by an oil-to-air cooler. The buffer air system prevents lubricating oil from entering the gas turbine. The generator and the electrical system are cooled by a separate cooling water system. As gas containing hydro carbons is highly flammable a fuel gas system is needed for safety reasons. If the delivery pressure of the natural gas is below 6 barg, the gas needs to be compressed to raise the pressure [7].

### 3.2.3 Turbec T100 at Risavika Gas Centre

The micro turbine stationed at Risavika Gas Centre is identical to the system described above. Due to research purposes it has some modifications. The combustion chamber is installed outside the casing of the Turbec and a bypass is connected to it, as illustrated by the stippled lines in Figure 3.2. By having the bypass it is possible to connect e.g. a fuel cell to the Turbec in order to replace the combustion chamber.

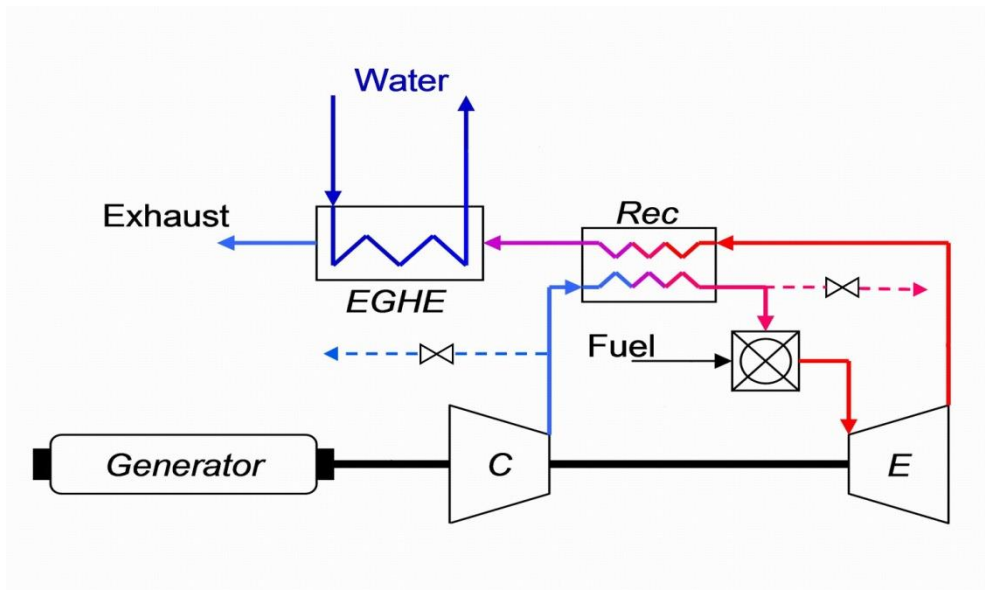


Figure 3.2 Process scheme of the Turbec T100 at RGC [Nikolett Sipöcz]

In addition to the measurement systems regarding surveillance and control of the Turbec, there are installed extra sensors measuring pressure and temperature for research matters. The sensors are U-bands installed after the compressor and before the combustion chamber and a tube inside the exhaust channel in the combustion chamber. This is illustrated in Figure 3.3. The sensors are connected to wire and tubes and then led to two data acquisition devices logging pressure and temperature [11]. The possible influence of these installations have on the performance of the Turbec at Risavika is not known at present.

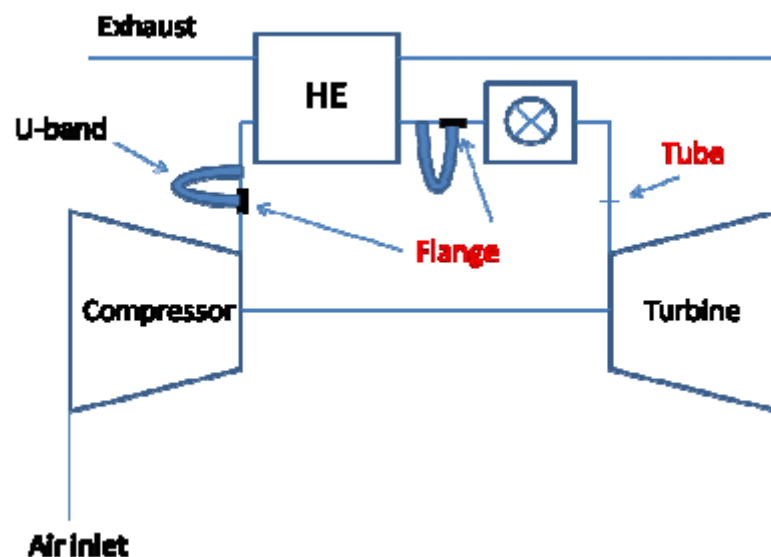


Figure 3.3 Scheme of the Turbec T100 at RGC with measuring locations [11]

## 4 Heat and Mass Balance Program

In order to make a thermal system analysis of a (heat and) power plant e.g. a gas turbine a heat and mass balance program (HMBP) is needed. In this chapter the concept of HMBP will be presented and there will be a further description of the HMBP IPSEpro.

### 4.1 General

The purpose of making a model is to describe the real world in a sufficient way that is less time consuming than calculating by hand. The model should not be more complicated than answering the problem of formulation. Both components and cycles containing a number of different components can be modeled by a HMBP. A HMBP uses laws of thermodynamics, i.e. the energy equation and the equation of conservation of mass, in order to calculate outputs of given inputs. Thus it is important that the user of HMBP has knowledge about thermodynamics and the characteristics of the components within the system. This in order to make accurate assumptions about pinch points, pressure losses, heat transfer coefficients, etc. The model could be of an existing system, but also un-existing systems could be modeled. When modeling an existing system, e.g. a gas turbine, there are given fixed parameters such as pressure ratio and turbine inlet temperature (TIT). In a non-existing system for which many parameters are unknown or unsure, a number of assumptions must be made [9].

HMBPs can either be commercial software packages, in-house coded, or software designed and distributed by the manufacturer of the power plant. The diversity and details of components included in the different HMBPs varies from software to software. The commercial software packages may have a wide variety of components but they could lack detailed specifications of the available components on the market. HMBPs delivered by a manufacturer of a certain engine, for monitoring and diagnosis purposes, the software could include a wealth of details. The way calculations are carried out also varies within different types of software. There are three different methods for calculating heat and mass balances; sequentially, simultaneous equation solving and a combination of the two called semi-parallel method. The sequential method calculates the variables in one component and the output data from this component is used as input data in the next, working its way through the whole series of components within the cycle. This makes it easier to model the cycle, but problems can occur when recirculated flows are present. The reason for this is when a cycle is closed the parameters where the cycle is linked together have to be equal. Hence, there will be an error in the mass balance if these parameters are unequal. If the simultaneous equation solving



method is applied then all the equations of all the components in the cycle is solved simultaneously after being gathered in a matrix. This requires accurate initial values and sufficient memory for the matrix [9].

## 4.2 IPSEpro

IPSEpro is a HMBP developed by SimTech and consist of modules for creating process models and for utilizing these models throughout the lifecycle of different kind of process plants. What makes IPSEpro stand out from other HMBPs is the ability to use components from either a standard library or to create new component models by using the model development kit.

### 4.2.1 Process Simulation Environment

Within the process simulation environment (PSE) a process model can be created based on components from a library [12], shown in Figure 4.1. The components are placed at the project flow sheet window and different data of the components used need to be specified e.g. the composition of the working medium, mass flow, ambient conditions, pressure ratio etc. If the model converges, i.e. no occurrence of errors or warnings, the results will be displayed in the flow sheet. In order to show how to model in IPSEpro and how the equations are solved an example is presented below, by a model setup of a gas turbine.

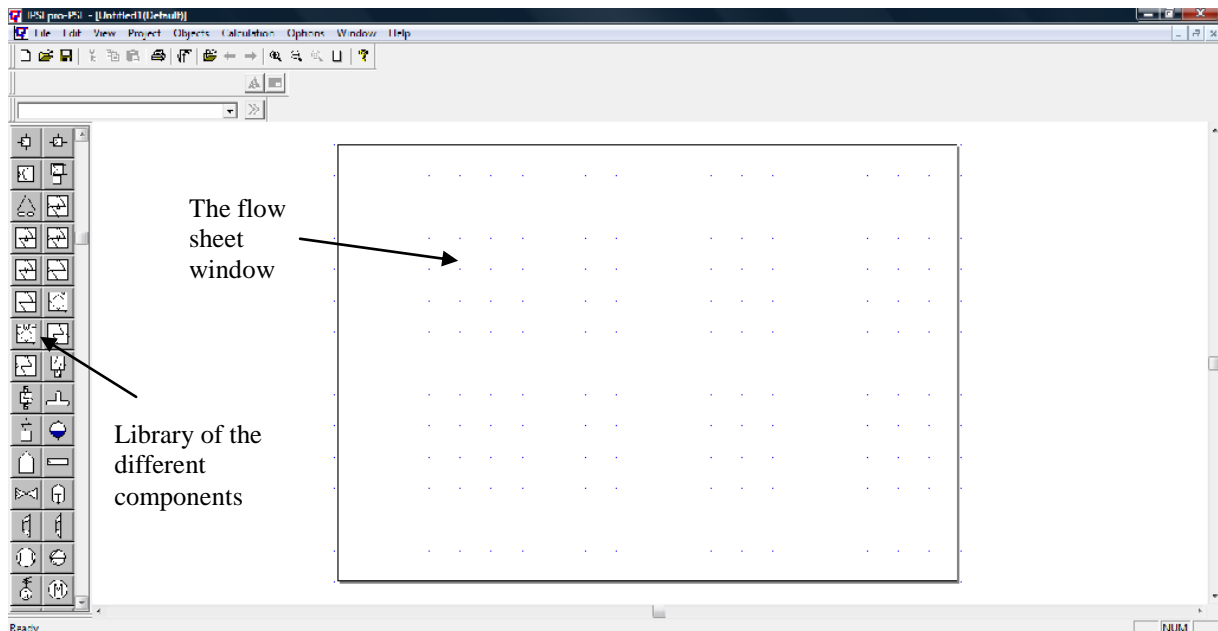


Figure 4.1 A screenshot of the PSE window

A compressor is added to the flow sheet window and the settings regarding pressure ratio, isentropic efficiency and mechanical efficiency are set as shown in Figure 4.2.

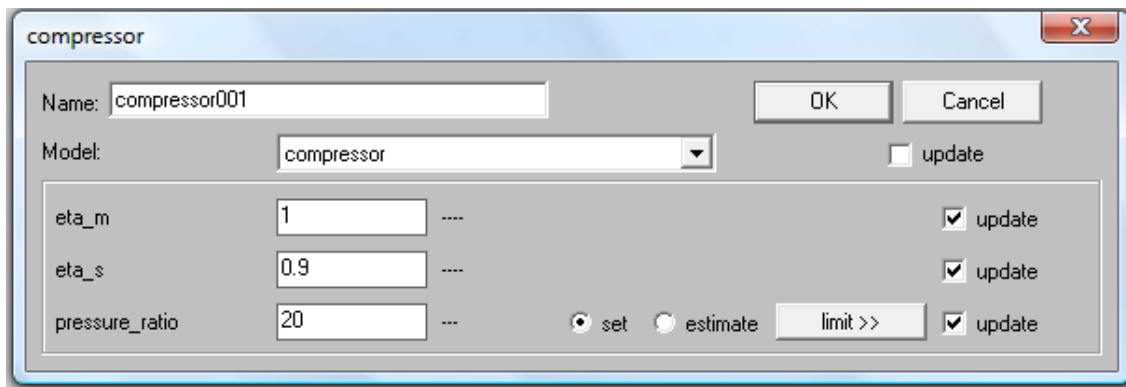


Figure 4.2 Settings of the compressor

Since air is the medium flowing inside the compressor, the composition of air must be defined. This is done by adding a new global object and editing it. The composition of air is in this example simplified and consists of 76 % Nitrogen and 24 % Oxygen. Now the ambient conditions of the air need to be set. As seen in Figure 4.3 the pressure is set to 1 bar, temperature to 15 °C and the mass flow rate to 50 kg/s

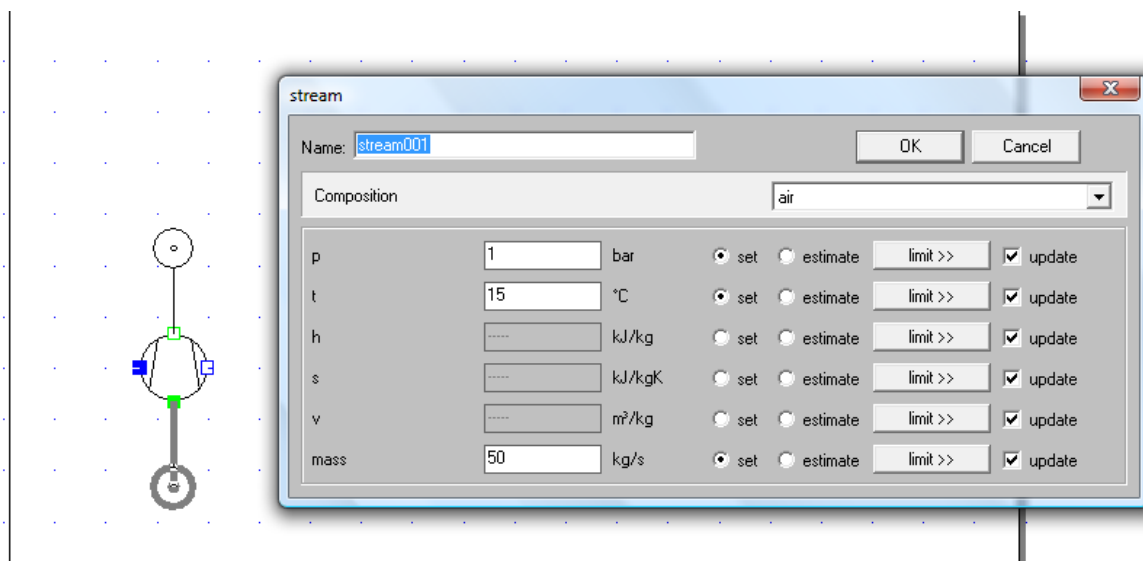


Figure 4.3 Settings of the ambient conditions

Now IPSEpro can calculate the data after the compressor. And the results are presented in the flow sheet as shown in Figure 4.4. By importing estimates PSE is adding results not shown in the flow sheet, such as specific volume and entropy. These values are shown in the component specification window or stream specification window as illustrated in Figure 4.3 for the stream entering the compressor.

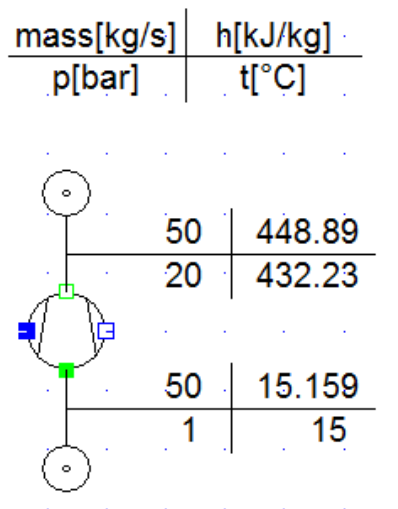


Figure 4.4 Results presented in the flow sheet

PSE uses thermodynamic laws to solve the equations. As there is no mass added in the compressor and the law of conservation of mass exists the mass flow rate is constant through during the compression. The pressure ratio was set to 20 and the ambient pressure was set to 1 bar, PSE then calculates the pressure out of the compressor to be 20 bars. By solving equation 2.5 in chapter 2.1.1 with respect to  $T_{02}$ , the outlet temperature of the compressor is calculated.

$$T_{02} = \frac{T_{01}}{\eta_c} \left[ \left( \frac{p_{02}}{p_{01}} \right)^{(\kappa-1)/\kappa} - 1 \right] + T_{01} \quad (4.1)$$

By adding a shaft to the compressor in the flow sheet PSE can calculate the power consumption. The calculation of the enthalpy is given by equation 2.3 in chapter 2.1.1.

$$W_c = \dot{m} \cdot (h_{01} - h_{02}) \quad (4.2)$$

$$W_c = -21\,687 \text{ kW}$$

After the compressor model converges, the combustion chamber can be added. The compressor and combustion chamber are connected as shown in Figure 4.5. There are three streams through the combustion chamber, air, fuel and exhaust gases. Air is already defined. The type of fuel needs to be specified, in this example it is natural gas, which in this case is simplified to 100 % methane ( $\text{CH}_4$ ). Inlet conditions of the fuel are specified to:  $T = 15 \text{ }^\circ\text{C}$ ,  $p = 2 \text{ bars}$  and  $m = 1 \text{ kg/s}$ . The composition of the exhaust gases is not known, and PSE will

calculate this according to the rules of stoichiometry. The pressure loss through the combustion chamber is set to zero.

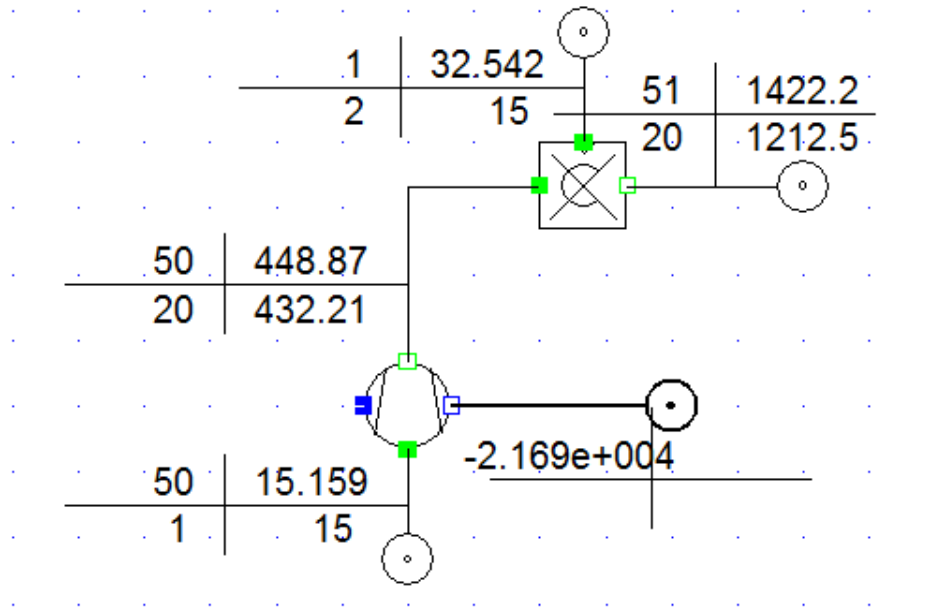


Figure 4.5 Compressor and combustion chamber linked together

When running the model now, eight warnings occur. To find out what the warnings are, it is possible to open a protocol where they are all listed.

```

=====
System solution finished.

%Warning: Test condition for composition Exhaust not satisfied:
tminWATER:      "WATER < 0.0"

%Warning: Test condition for composition Exhaust not satisfied:
tminAR: "AR < 0.0"

%Warning: Test condition for composition Exhaust not satisfied:
tminC2H6:      "C2H6 < 0.0"

%Warning: Test condition for composition Exhaust not satisfied:
tminC3H8:      "C3H8 < 0.0"

%Warning: Test condition for composition Exhaust not satisfied:
tminCH4:      "CH4 < 0.0"

%Warning: Test condition for composition Exhaust not satisfied:
tminCO: "CO < 0.0"

%Warning: Test condition for composition Exhaust not satisfied:
tminSO2:      "SO2 < 0.0"

%Warning: Test condition for combustor_c combustor_c001 not satisfied:
t_delta_p_comb: "fuel pressure must be >= main stream pressure"

```

Figure 4.6 List of warnings

As seen in Figure 4.6 seven of the warnings regard the composition of the exhaust gases. PSE has calculated some of the exhaust gases to have negative mass-%. This is physically impossible. To get rid of the warnings limiting values of the exhaust gases need to be set. Since the mass-% is negative, the limit is set to go from zero to one. Running the model now the exhaust gases that had negative mass-% are estimated to be zero, and there is only one warning left. This warning regards the inlet pressure of the fuel. The value of the fuel pressure is less than the pressure of compressed air. When this is the case the fuel will not enter the combustion chamber. Thus the pressure of the fuel needs to be changed to a higher value than the pressure of the compressed air. The fuel pressure is now changed to 25 bars, and the model converges, and the results are presented as shown in Figure 4.7. The mass flow rate is increased to 51 kg/s as a result of the fuel added to the cycle.

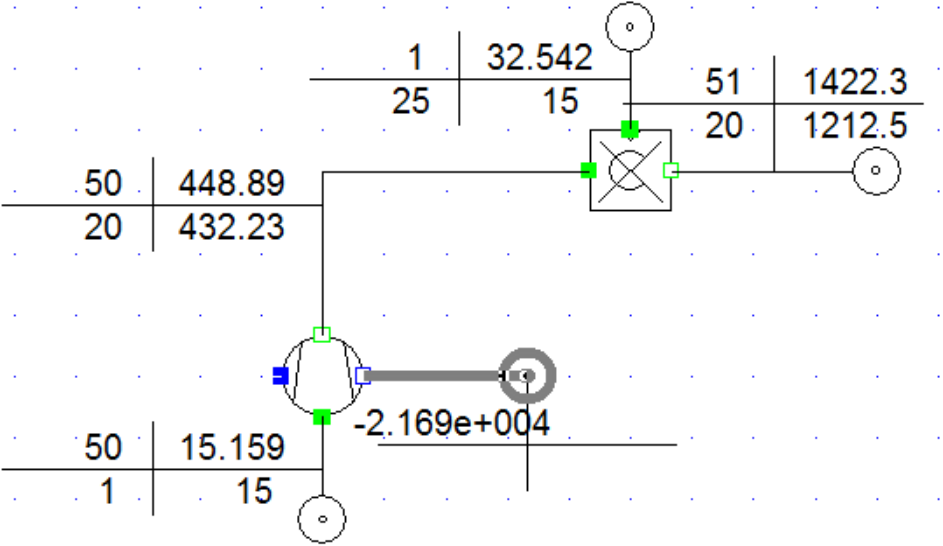


Figure 4.7 Compressor + combustion chamber

The turbine can now be added to the cycle. The isentropic efficiency is set to 0,9, the mechanical efficiency is set to 1, pressure of the exhaust gases leaving the turbine is assumed to 1 bar. IPSE calculates the temperature out of the turbine by solving equation 2.6 in chapter 2.1.1 with respect to  $T_{04}$ .

$$T_{04} = T_{03} - \eta_t T_{03} \left[ 1 - \left( \frac{1}{p_{03}/p_{04}} \right)^{(\kappa-1)/\kappa} \right] \tag{4.3}$$

The shaft of the compressor is connected to the turbine and is then connected to a generator, as shown in Figure 4.8. The mechanical efficiency of the generator is set to 1 and the electrical efficiency is set to 0,98.

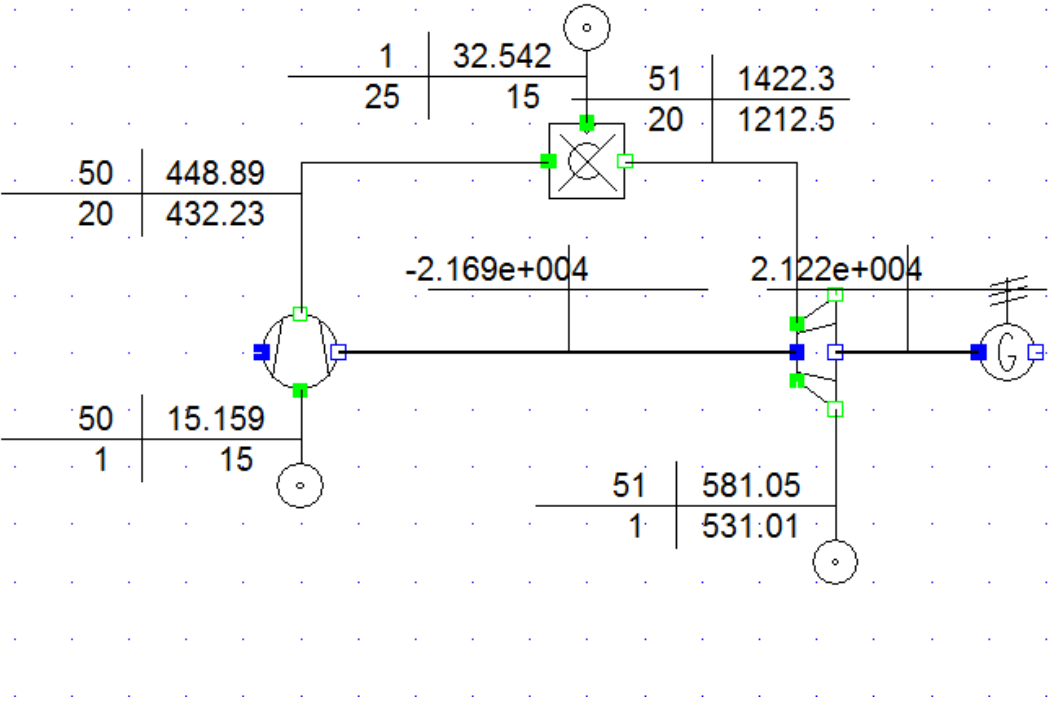


Figure 4.8 Model of a gas turbine cycle

The work produced by the turbine is calculated by the program according to equation 4.4

$$W_t = \dot{m}(h_{03} - h_{04}) \tag{4.4}$$

Resulting in a work output of

$$W_t = 42\,903,75 \text{ kW}$$

As the turbine drives the compressor 21 215 kW goes to the generator, and the electrical efficiency is 0,98 giving a net power output of 20 791 kW, as shown in Figure 4.9.

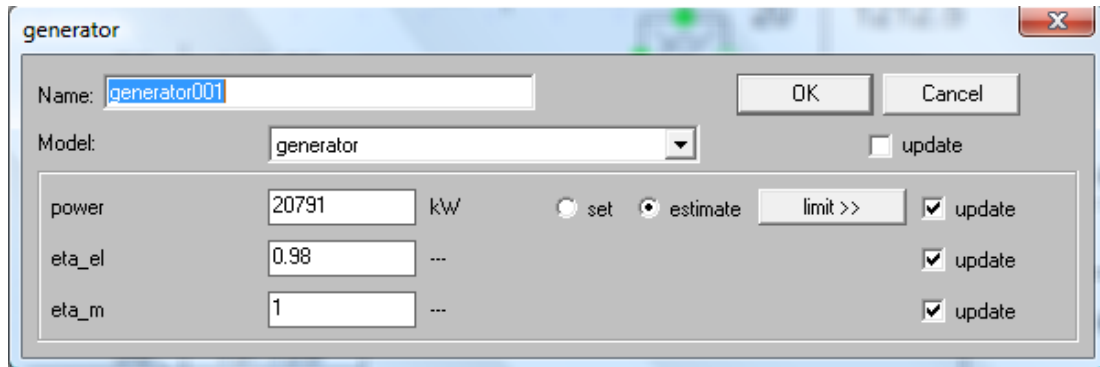


**Figure 4.9 Generator settings and output**

The total efficiency of the gas turbine can now be calculated by utilizing equation 2.12 presented in the previous chapter 2.1.3.

$$\eta_{total} = \frac{W_{out}}{Q_{in}} = \frac{W_{out}}{(\dot{m}_2 \cdot h_{03}) - (\dot{m}_1 \cdot h_{02})} \quad (4.5)$$

$$\eta_{total} = \frac{20\,791}{(51 \cdot 1422,3) - (50 \cdot 448,89)}$$

$$\eta_{total} = 0,415 = 41,5 \%$$

As seen in Figure 4.8 the temperature out of the compressor is lower than the turbine outlet temperature. Thus a recuperator can be useful and improve the total efficiency of the gas turbine. A counter flow heat exchanger is selected from the library and inserted between the compressor and combustion chamber, as shown in Figure 4.10. The *pinch point out* is set to 10 °C and the pressure losses through the recuperator is set to zero. *Pinch point out* is the difference between the temperature leaving the turbine and the temperature of the air entering the combustion chamber. Instead of setting the mass flow rate of the fuel the TIT is set equal to the temperature calculated by IPSE in the previous example. This way the performance and efficiency of the two cycles can be compared.

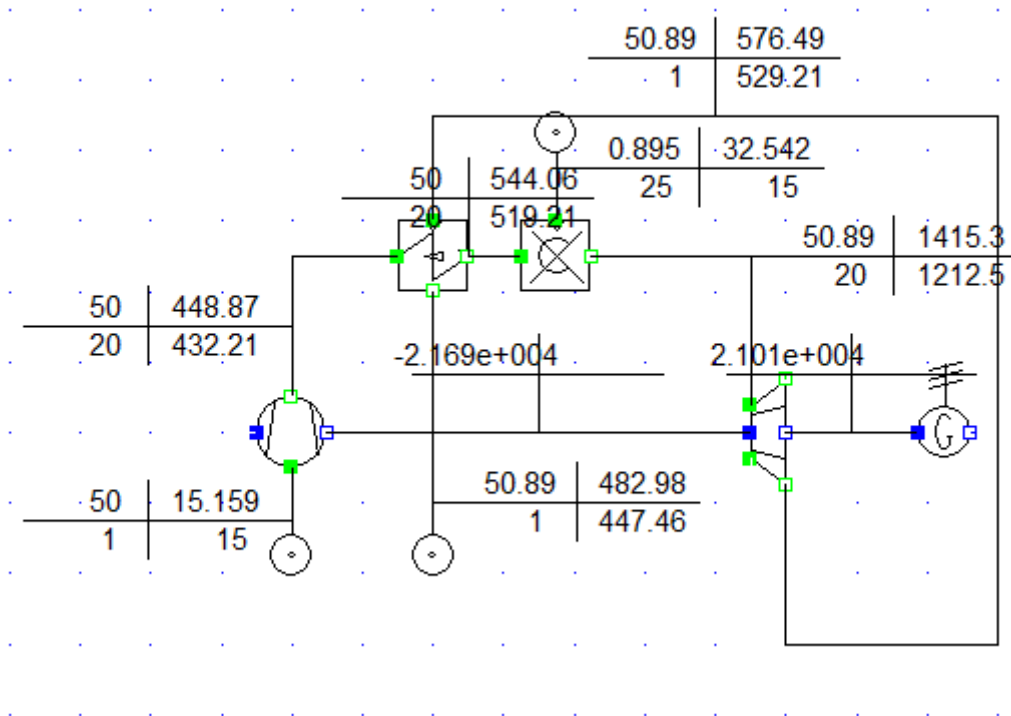


Figure 4.10 The gas turbine with a recuperator installed

The power output of this cycle is 20 585 kW, this is a little less power produced than the regular gas turbine cycle in the previous example. The reason for this is that less fuel is needed in order to obtain a TIT of 1212,5 °C and hence the mass flow rate of the exhaust gases are reduced. The efficiency on the other hand is increased to 46,6 %.

#### 4.2.1.1 Calculation Method

PSE calculates equations by the semi-parallel method, a combination of the sequential and simultaneous method. The equations for one component are gathered in one matrix and solved simultaneous. The output data from the first component are used as input data in the next component and the equations for this component are gathered in a new matrix and so it continues throughout the cycle. If some of the equations remain unsolved they are gathered in one last matrix and solved. The equations are iterated by numerical methods in order to give accurate solutions. PSE uses the optimum numerical method for a given equation. If the equation does not converge by the chosen numerical method PSE tries a new method. What numerical method PSE chooses to use is not known to the user of the software. An example of a numerical method is the Newton-Raphson method. With this approach PSE iterate the variable,  $x_o$ , that was calculated sequentially by,



$$x_1 = x_0 - \frac{f(x_0)}{f'(x_0)} \quad (4.6)$$

Where  $f(x_0)$  is the equation solved by variable  $x_0$  and  $f'(x_0)$  is the derivate equation solved by the variable  $x_0$ .

The process is repeated until a sufficient accurate value is reached:

$$x_{n+1} = x_n - \frac{f(x_n)}{f'(x_n)} \quad (4.7)$$

The number of iteration steps and accuracy can be determined by the user of the software as shown in figure 4.11.

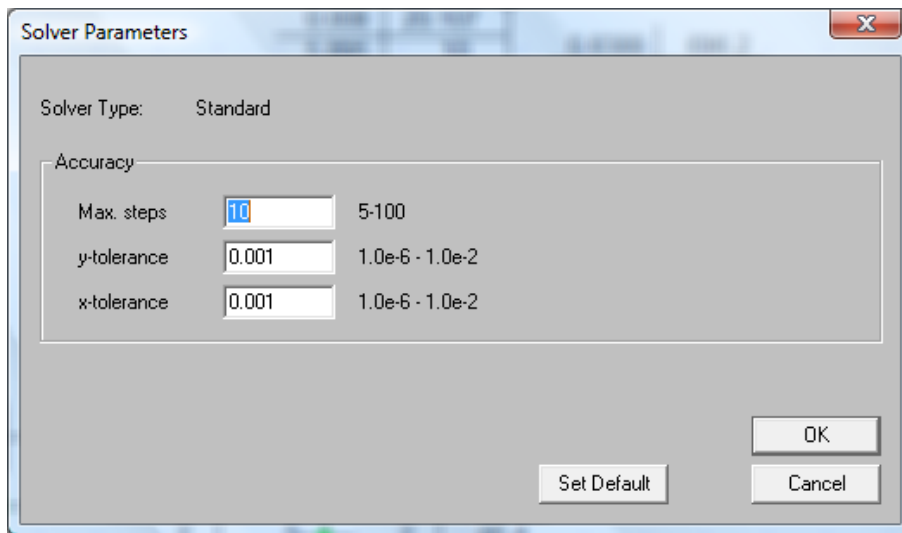


**Figure 4.11** Number of iteration steps and accuracy

If the criteria in Figure 4.11 are not fulfilled, PSE will display an error message in the protocol.

Other errors that can occur are when the system of equations is structurally singular, the system of equations is numerically singular and when there are errors in the built-in or external numerical functions [10].

When the system of equations is structurally singular, the system of equations either is over defined or undefined. A system is over defined when the system contains more equations than variables. PSE will solve the equations and present the results if the over defined constant is equal the one calculated by PSE. However, a warning will be published in the protocol. If the over defined constant is different from the one estimated by PSE an error will occur. This is

illustrated by the example of the gas turbine modeled above in Figure 4.12. In this case the pressure ratio is set to 20 and the pressure after the compressor is set to 21 bars. As the inlet pressure is 1 bar PSE want to calculate the outlet pressure to 20 bars, due to the setting of 21 bars the error occurs and the results are blue instead of black.

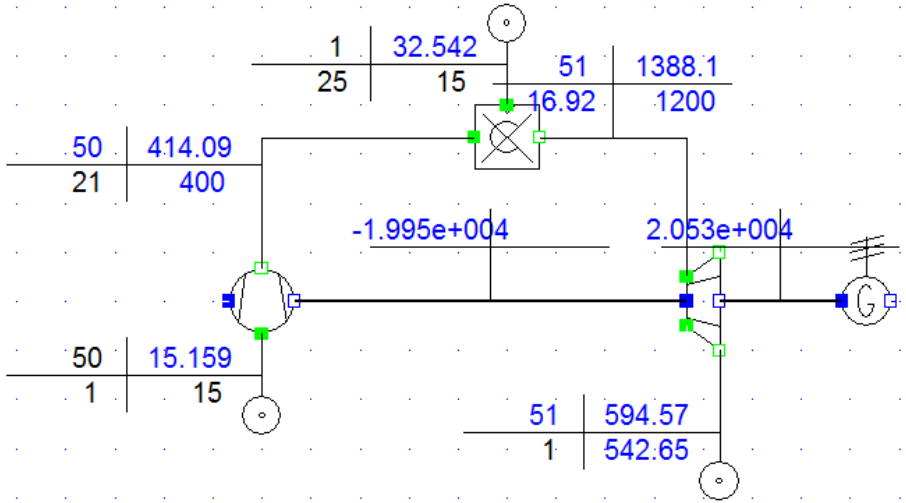


**Figure 4.12 The gas turbine cycle is over defined**

A system is undefined when there are more variables than equations in the system. In the case shown in Figure 4.13 no pressure ratio or pressure after the compression is set. PSE cannot solve the equations because of the lack of information regarding the pressure ratio in the compressor. If the protocol is opened it says that the problem is undefined and there are 45 equations and 46 variables. There are three approaches in order to solve this problem:

1. Set the pressure ratio in the compressor
2. Set the pressure after the compressor or combustion chamber
3. Set the temperature after the compressor or combustion chamber

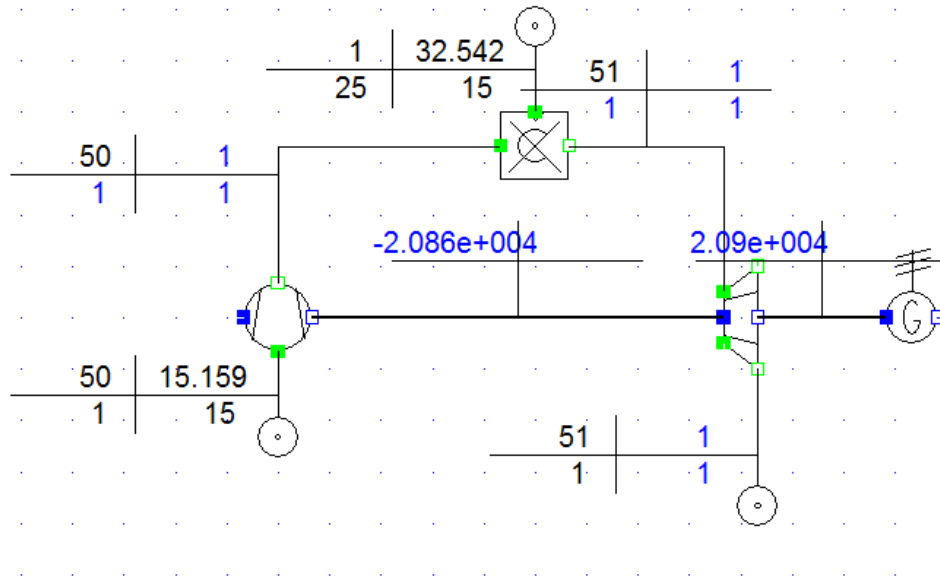


**Figure 4.13** The gas turbine cycle is undefined

#### 4.2.2 PSExcel

PSExcel is a module that allows data exchange between PSE and MS-Excel i.e. data from a PSE project can be incorporated in a excel worksheet [12], as shown in Figure 4.14.

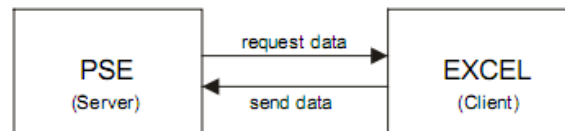


**Figure 4.14** Scheme of data exchange between PSE and Excel [12]

PSExcel is an Excel worksheet containing the necessary macros in order to make variations from the model created in PSE and publish the results in an Excel worksheet. The simulation could either be two- or three-dimensional i.e. a variation of one or two parameters simultaneously, as shown in Figure 4.15.

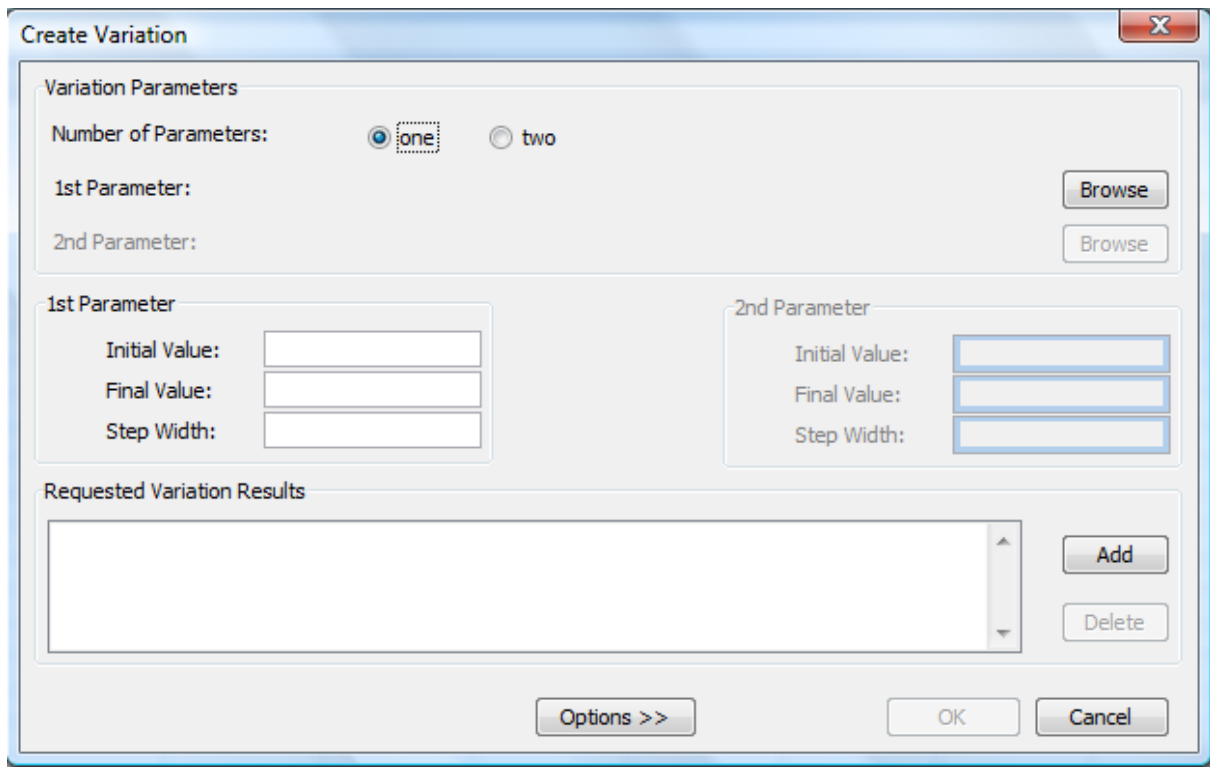


**Figure 4.15 Creating a variation in PSEExcel**

After the number of parameters has been selected, the parameter(s) need to be defined. As an example in Figure 4.16 ambient temperature is chosen to be the varied parameter.

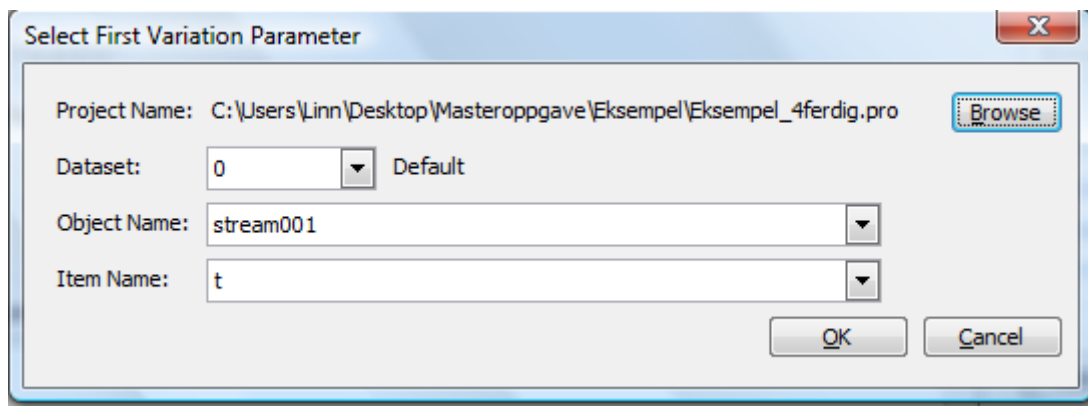


**Figure 4.16 Selecting variation parameter**

When the parameter is defined, the boundary conditions for the variation need to be set. As seen on Figure 4.15 the required data for the variation is listed i.e. initial value, final value and step width. In this example it will be shown how the performance of a gas turbine changes with changes in ambient temperature. The compressor inlet temperature i.e. ambient temperature is varied between  $-15\text{ }^{\circ}\text{C}$  and  $25\text{ }^{\circ}\text{C}$  and with a step width of  $5\text{ }^{\circ}\text{C}$ . Then the output data must be requested. In order to show the performance of the gas turbine in terms of efficiency it is desirable to request power output from the generator, heating value of the fuel

and mass flow rate of the fuel. Now the simulation can be started, and the results are presented in the excel worksheet as shown in Figure 4.17.

Data-Set: 0  
 Parameter: stream001.t  
 Initial Value: -15  
 Final Value: 25  
 Step Width: 5

stream001.t	combustor_c001.heating_value	stream003.mass	generator001.power
-15	50042,53711	1	21268,40279
-10	50042,53711	1	21188,82433
-5	50042,53711	1	21109,06158
0	50042,53711	1	21032,12423
5	50042,53711	1	20952,56829
10	50042,53711	1	20873,05295
15	50042,53711	1	20793,65453
20	50042,53711	1	20714,3811
25	50042,53711	1	20635,23532

Figure 4.17 Results from the variation

These results can be plotted in a graph as shown in Figure 4.18. As described in chapter 2.1.4, about ambient conditions, the power produced by the gas turbine decreases with increased temperature.

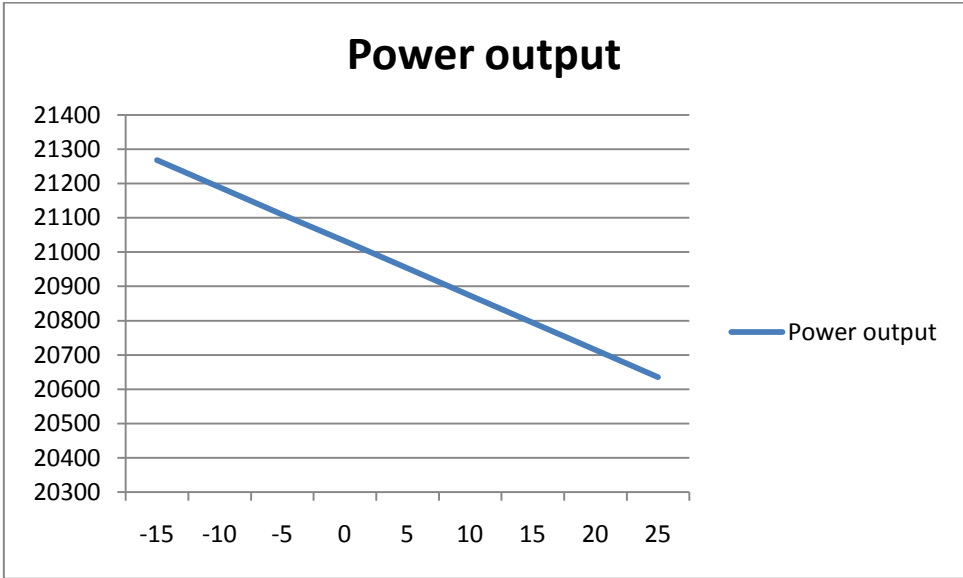


Figure 4.18 Temperature and power output plotted in a graph

By dividing the power output by the heating value and mass flow rate, the total efficiency of the gas turbine is determined.

### 4.2.3 Model Development Kit

What makes IPSEpro stand out from many other HMBPs is that the user has access to the source code of the models and is able to modify or create new models by the Model Development Kit (MDK). IPSE component models can be divided into three main groups: Units, connections and globals. Units are the actual components where thermodynamic changes take place for example heat exchangers, turbines and compressors. Connections are the nodes linking linking the units and are sources where thermodynamic states are calculated. Globals are the composition of the media flowing through the units and connections e.g. steam, air and exhaust gases [15].

The model development tool provides the functionality to build new model libraries that match specific application requirements [13]. As an example the gas turbine in the standard library only takes the isentropic efficiency into account. By modifying the gas turbine in MDK the performance of the gas turbine could be presented by means of the polytropic efficiency. After the model is modified in MDK it can be used in PSE. MDK provides a model description language (MDL) to describe models mathematically. This is an equation oriented language i.e. the sequence of equations within the model has no influence on how the equations are processed.

### 4.2.4 Identification of HMB Equations Relevant for Validation Purposes

Since a model of a Turbec T100 is going to be validated in this thesis it is necessary to identify which HMB equations are relevant for this validation process. These equations are presented Table 4.1.

Components	Equations	Comments
Compressor	$p_{02} = p_{01} \cdot \pi$	$\pi$ = pressure ratio
	$m_{02} = m_{01}$	Conservation of mass
	$h_{02} - h_{01} = \frac{(h_{02}' - h_{01})}{\eta_c}$	
	$\frac{(h_{02} - h_{01}) \cdot m_{01}}{\eta_m} = P_{shaft c}$	The temperature is defined by the enthalpy

Combustor	$m_{03} = m_{01} + m_{fuel}$	
	$p_{03} = p_{02} - \Delta p$	Pressure loss through the combustion chamber
Turbine	$m_{04} = m_{03}$	Conservation of mass
	$h_{03} - h_{04} = (h_{03} - h_{04r}) \cdot \eta_T$	
	$(h_{03} - h_{04})\eta_m \cdot m_{03} = P_{shaft T} - P_{shaft C}$	
Heat exchanger	$m_{02 cold} = m_{02 hot}$ $m_{04 hot} = m_{04 cold}$	Conservation of mass
	$p_{02 hot} = p_{02 cold} - \Delta p$ $p_{04 cold} = p_{04 hot} - \Delta p$	Pressure loss
	$T_{02 hot} = T_{02 cold} + \Delta T_{cold}$ $T_{04 cold} = T_{04 hot} - \Delta T_{hot}$	Temperature change

**Table 4.1 HMB equations**

There exist more equations within IPSEpro than those listed in Table 4.1.

For further reading about all the equations the reader is referred to SimTech [[www.simtechnology.com/english/SimTech.php](http://www.simtechnology.com/english/SimTech.php)].

## 5 Modeling Turbec T100

This chapter describes how the Turbec T100 was modeled and which data was generated for further processing.

The model of the Turbec T100 is based on the process scheme illustrated in Figure 5.1.

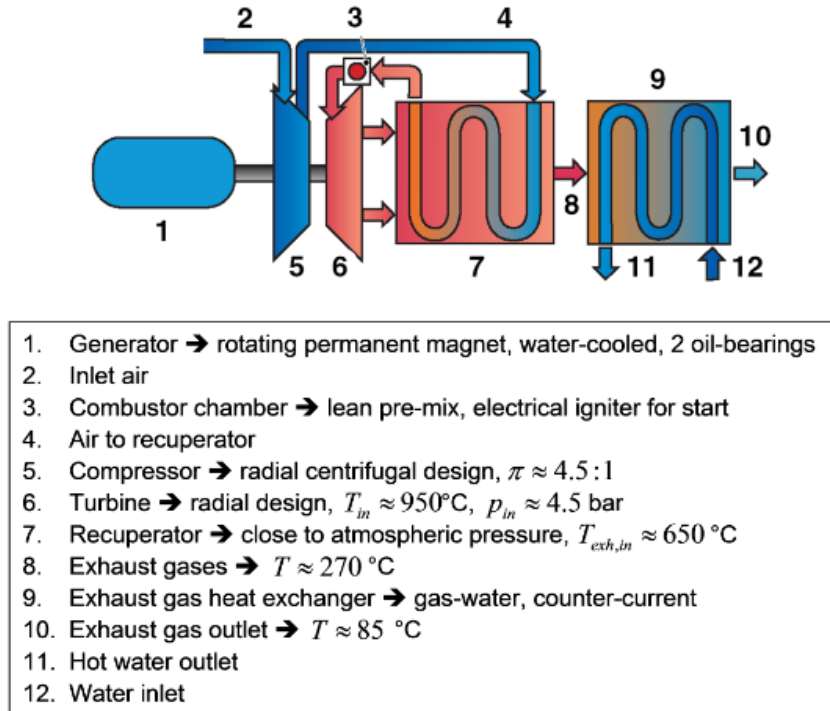


Figure 5.1 Process Scheme of Turbec T100

At first the pressure ratio,  $\pi$ , was set to 4,5:1, TIT was set to 950 °C and the turbine outlet temperature was set to 650 °C, along with the assumptions presented in Table 5.1.

Table 5.1 Assumptions implemented in the model

	Assumptions
Ambient temperature	15 °C
Ambient pressure	1,013 bar
Ambient relative humidity	60 %
Pressure drop HTX	0,022 bar
Pinch point out HTX	82 °C
Pressure drop combustion chamber	0
Mass flow rate after expansion	2,016 kg/s

Comparing the power output with a standard Turbec T100, which produces 100 kW, revealed that the power output was too low. Instead of setting the turbine outlet temperature, the



isentropic efficiency of the turbine was set to 84,1 %, resulting in a better power output. The fuel flow was not known and the exhaust gas mass flow rate was set to 2,016 kg/s, which was realized to be somewhat overestimated.

As seen in Figure 5.1 the Turbec T100 is installed with a counter flow heat exchanger, for heating up water purposes as the unit is of CHP type. The Turbec T100 is modeled as described in chapter 4.2.1, and the heat exchanger is included as part of the system. Figure 5.2 shows the model set-up of the Turbec T100 in IPSEpro.

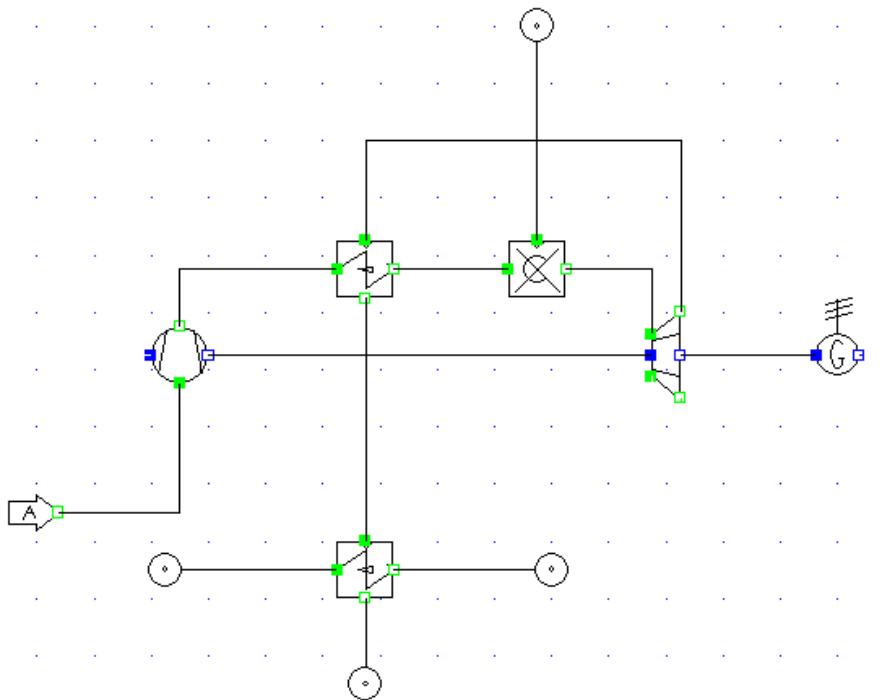


**Figure 5.2 Modeled Turbec T100 containing a counter flow heat exchanger**

This model was initially made for generating data, by using PSEExcel, for Mats Mathisen's Master Thesis, *Noise Filtering from a Nonlinear System by Using AANN*. The parameters varied were: ambient pressure, ambient temperature and relative humidity and the variation were done in three dimensions, i.e. varying two parameters simultaneously, as illustrated in Table 5.2.

**Table 5.2 Parameters of variation**

Variation no.	Constant	Varying parameter 1	Varying parameter 2
1	Relative humidity	Ambient pressure	Ambient temperature
2	Ambient pressure	Relative humidity	Ambient temperature
3	Ambient temperature	Relative humidity	Ambient pressure

The ambient pressure was varied from 0,975-1,04 bar and a step width of 0,001 bar. The temperature was varied from -15-25 °C with a step width of 0,5 °C. The relative humidity was varied from 35-90 % with a step width of 1 %. These variations generated a total amount of 13 578 data patterns. The requested output data were: mass flow rate out of the compressor, compressor outlet pressure, compressor outlet temperature, fuel flow, turbine outlet temperature, turbine outlet pressure, generator power and shaft power required by the compressor. The results were organized in an excel-sheet and sent to Mats Mathisen for further processing.

## 6 Validation of the Turbec T100 Model

The validation of the IPSE model of Turbec T100 described in previous chapter 5 has been made using real data from the microturbine installed at Risavika. Measurements during four days of continuous operation (2010-04-19-21010-04-23) of the Turbec at Risavika was gathered and further analysed in order to be used in the validation work. The measured values from the Turbec were then inserted in the HMB model, and thereafter the power output from the model was compared to the power output measured at Risavika. By doing this the isentropic efficiencies of both compressor and turbine could be found. These are values that are currently not known.

The validation is based on measurements from the Turbec T100 when it is operating at full load. The reason for only looking at the Turbec's performance when operating at full load is because this model in IPSEpro does not take the number of revolutions into account, i.e. it is modeled when operating at full load.

There have been three systems taking measurements during the time period of continuous operation: The SCADA-system, Turbec's internal system and the additional system (described in chapter 3.2.3), now referred to as the AC-flow system.

In this chapter all the input data implemented into the IPSE model will be presented.

### 6.1 Composition of the Natural Gas

At first the composition of the natural gas need to be known. The typical composition is given by Lyse AS and is presented in Table 6.1.

**Table 6.1 Composition of the natural gas**

Name	Chemical formula	Mol %
Methane	CH <sub>4</sub>	88,36
Ethane	C <sub>2</sub> H <sub>6</sub>	8,49
Propane	C <sub>3</sub> H <sub>8</sub>	0,35
Carbon dioxide	CO <sub>2</sub>	2,03
Nitrogen	N <sub>2</sub>	0,77
Total		100

As IPSE operates with mass fractions instead of mol fractions, the composition is converted into mass fractions. This is done by multiplying the molar mass to each of the elements within the composition. Now the mass of one mol for each element is found. The mass fractions are

simply found by dividing the mass of each element with the total mass. The results are presented in Table 6.2.

**Table 6.2 Conversion of mol fractions to mass fractions**

Name	Chemic Formula	Mol fraction	Molar mass	Mass	Mass fraction	Approx. Mass fraction
			kg/kmol	Kg		
Methane	CH4	0,8836	16.043	14,1755948	0,78788407	0,7877
Ethane	C2H6	0,0849	30.07	2,552943	0,14189338	0,142
Propane	C3H8	0,0035	44.097	0,1543395	0,00857824	0,0086
Carbondioxide	CO2	0,0203	44.01	0,893403	0,04965562	0,0497
Nitrogen	N2	0,0077	28.013	0,2157001	0,01198868	0,012
Total		1	162.233	17.9919804	1	1

## 6.2 Ambient Condition Measurements

Ambient pressure and relative humidity are currently not measured at Risavika. The ambient conditions during the period are based on on measurements by, senior scientific officer, Kåre Bærheims weather station installed at University of Stavanger. The weather conditions at University of Stavanger are assumed to be the same as at Risavika. The frequency of these measurements was every half hour.

## 6.3 SCADA-system measurements

The SCADA system is measuring the fuel flow, this is measured in  $\text{Nm}^3/\text{h}$  and is converted to  $\text{kg/s}$  by the density  $\rho = 0,84 \text{ kg}/\text{Nm}^3$  given by Lyse AS. The frequency of these measurements was every minute. It is given by RGC that the pressure of the fuel can be set to 5 bars and a temperature set to  $80 \text{ }^\circ\text{C}$ .

## 6.4 Turbec Internal Measurement System

Turbec's internal system is measuring the power output and the turbine outlet temperature. Based on the turbine outlet temperature the internal system estimates the turbine inlet temperature. There are more measurements done by the internal system, but these were not relevant for this thesis. The frequency of these measurements is approximately every one and a half minute.

## 6.5 AC-flow Measurements

The AC-flow system measures the compressor outlet temperature, compressor outlet pressure, the pressure after the recuperator, turbine inlet pressure and turbine inlet temperature. The measuring frequency was 12 times a minute.

## 6.6 Synchronization of the Measured Data

There is installed a cooling valve between the combustion chamber and turbine, in order to cool the combustion chamber and the measuring probe. The pressure of the cooling air is approximately 4,5 bars. When the valve is open it has an effect on the measuring flange in this area i.e. the pressure is increased after the combustor. In order to get accurate measurements of TIT and turbine inlet pressure the valve had to be closed. Two times a day the valve was closed for a time period of approximately five minutes when the Turbec was operating at full load, as shown in Table 6.3. The five minutes when the cooling valve was closed was located in the Ac-flow excel work sheet when the pressure after the combustion chamber decreased to approximately 3,4 bars and the TIT was at its highest, approximately 800 °C.

**Table 6.3 Time periods for when the cooling valve was closed**

	from	to	
Date	time	time	Load
20.apr	08:30	08:35	50 kW
20.apr	10:27	10:32	50 kW
20.apr	12:29	12:34	75 kW
20.apr	14:31	14:36	75 kW
21.apr	08:29	08:34	100 kW
21.apr	10:33	10:38	100 kW
21.apr	12:26	12:31	75 kW
21.apr	14:31	14:36	75 kW
22.apr	08:30	08:35	100 kW
22.apr	10:30	10:35	100 kW
22.apr	12:30	12:35	75 kW
22.apr	14:52	14:57	75 kW
23.apr	08:27	08:32	100 kW
23.apr	10:27	10:32	100 kW
23.apr	12:27	12:32	50 kW

As seen in the previous subchapters, the frequency of how many measurements are taken within one time period differs from each system. In Table 6.4 below, the measuring system, the frequency of the measurements and which relevant values measured are listed.

**Table 6.4 Frequency of the measurements**

System	Frequency of measurements	What is measured
Weather station at UiS	Every half hour	Amb. temperature, amb. pressure and amb. relative humidity
SCADA-system	Every minute	Fuel flow
Turbec's internal system	Approximately every 1,5 minutes	TOT, TIT calculated by the system with regard to TOT and the power output
AC-flow system	12 times a minute, i.e. every 5. second	COP, COT, pressure after HTX, TIP and TIT

By knowing the time when the measurements started and the frequency of the measurements taken it was possible to insert all the measurements in a excel work sheet with the corresponding time. In the AC-flow system where the frequency was 12 times a minute, an average of the values within one minute was calculated.

The date did not correspond between the measurements from the internal system and the AC-flow system. The excel work sheet containing measurements from the internal system had a date set to 2007.10.31. RGC had not set the correct date for the measurements in Turbec's internal system to 2010.19.04. The time for the measurements did not correspond either. Thus it was necessary to locate when the microturbine was operating at full load by plotting the power output and the pressure out of the compressor, as shown in Figure 6.1 and 6.2 correspondingly.

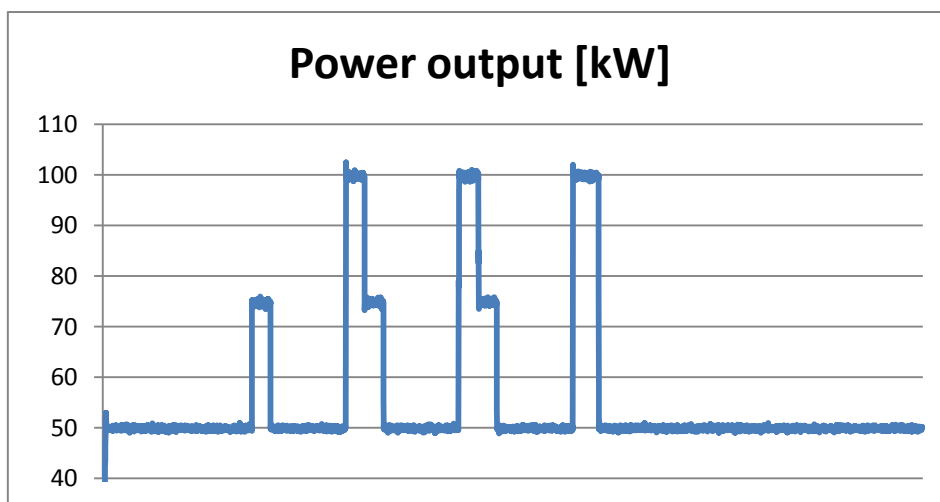


**Figure 6.1 Power output given by the internal system on the Turbec T100**

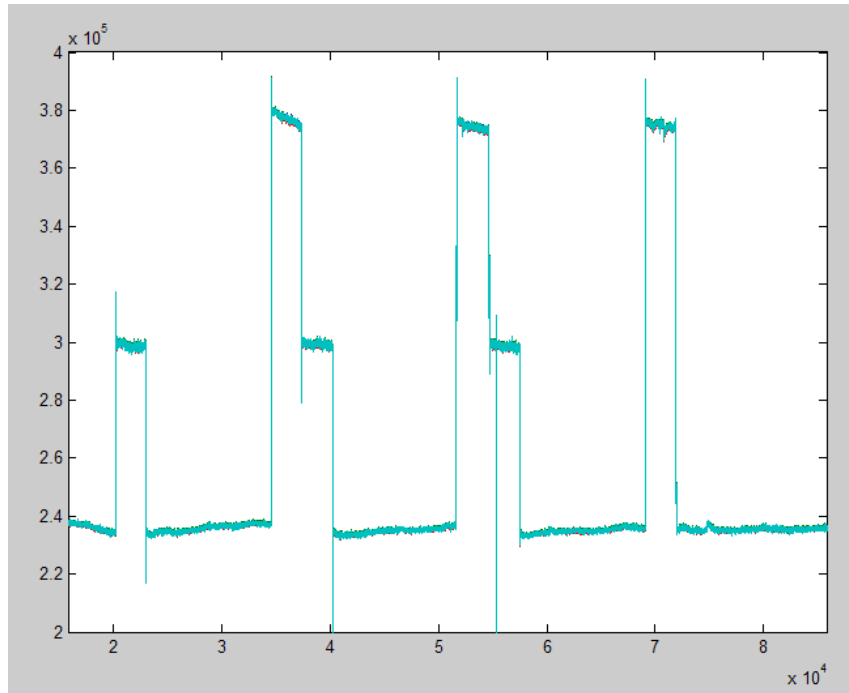


**Figure 6.2 Compressor outlet pressure given by the additional system**

As seen in Figure 6.1 and Figure 6.2 the peaks of the power output correspond with the peaks of the compressor outlet pressure, and the date and time can then be found. When the Turbec T100 operates at full load i.e. produces 100 kW, the compressor outlet pressure is approximately 3,8 bars, or  $3,8 \cdot 10^5$  Pa as illustrated in Figure 6.2 (the three highest peaks).

All the data from the each of the measurements was inserted in an excel work sheet resulting in a total of 36 full load measurements. All the measurements relevant for this thesis are presented in the Appendix.

## 7 Results and Discussion

In this chapter results from the validation will be presented and discussed.

The model is validated by choosing two groups of measurements for each time period, i.e. when the cooling valve was closed. This resulted in a total of 12 groups of data inserted in to the model as shown in Table 7.1. As the isentropic efficiency for the compressor is a value that needs to be set in IPSE, the compressor outlet temperature (COT) is an approximation to the measured value. The measured value is approximately 209 °C, which is a relatively high. By trying different isentropic efficiencies for the compressor with respect to the COT, the value was determined to be 61 %. By inserting all the values in Table 7.1 and set the isentropic efficiency for the compressor, the model converges and the power output is calculated. The results are presented in Table 7.2. This particular case will be referred to as case 1.

**Table 7.1 Measurements from RGC inserted in the model**

no.	Amb. P	Amb. T	Amb. Phi	Fuel flow	COP	Delta P HTX	TIP	TIT	TOT
	bar	C	%	kg/s	bar	bar	bar	C	C
1	1.007	2.5	92	0.0083871	3.8000411	0.2134798	3.4614396	822.7448940	615.5
2	1.007	2.5	92	0.0083861	3.7985556	0.2141101	3.4587796	817.2043132	615.4
3	1.0083	4.5	81	0.0083557	3.7729319	0.2128716	3.4353320	816.7686080	624.7
4	1.0083	4.5	81	0.0083555	3.7749543	0.2134985	3.4368863	793.6541990	624.5
5	1.012	4.6	83	0.0082823	3.7601003	0.2092572	3.4238825	809.5816946	623.1
6	1.012	4.6	83	0.0082792	3.7624921	0.2097367	3.4253456	788.8431978	624.4
7	1.012	5.8	67	0.0082259	3.7436743	0.2087286	3.4083090	806.4654064	627.5
8	1.012	5.8	67	0.0082238	3.7477726	0.2085884	3.4120430	746.2097072	627.0
9	1.0087	3.1	80	0.0083379	3.7614633	0.2081082	3.4247249	779.3308019	618.2
10	1.0087	3.1	80	0.0083374	3.7633970	0.2087424	3.4263818	777.7159590	618.4
11	1.0092	4.4	63	0.0083022	3.7477975	0.2076547	3.4133043	810.7521321	621.6
12	1.0092	4.4	63	0.0082996	3.7293005	0.2077706	3.3940262	773.8498973	621.3



**Table 7.2 Results from the calculation**

no.	Power	eta_sturb	m2	h2	m3	h3	Efficiency Turbec
	kW		kg/s	kJ/kg	kg/s	kJ/kg	
1	-2.5112	0.71907	1.2035	580.68	1.2119	900.2	-0.640442332
2	-8.7363	0.70373	1.2294	580.57	1.2378	893.37	-2.228303323
3	-20.162	0.67356	1.2708	590.9	1.2792	892.39	-5.161411642
4	-52.153	0.6044	1.4025	590.68	1.4109	864.02	-13.3514374
5	-25.754	0.6593	1.2898	589.12	1.2981	883.62	-6.651684046
6	-57.449	0.59134	1.4199	590.57	1.4281	858.14	-14.8462607
7	-35.561	0.63645	1.3219	593.73	1.3301	879.16	-9.248176896
8	-145.5	0.44593	1.7763	593.17	1.7846	805.87	-37.84059156
9	-62.816	0.58386	1.4552	583.4	1.4636	846.4	-16.11379971
10	-65.905	0.57795	1.4675	583.62	1.4758	844.42	-16.91030862
11	-22.256	0.66917	1.2805	586.88	1.2888	884.25	-5.734285928
12	-75.853	0.55894	1.5083	586.55	1.5166	839.16	-19.55091678

In Table 7.2 eta\_sturb is the isentropic efficiency of the turbine, m2 and h2 are the mass flow and the enthalpy of the air entering the combustion chamber and m3 and h3 are the mass flow and enthalpy of the gas leaving the combustor.

As seen in Table 7.2 it appears that the Turbec is a power consuming unit instead of a power producing unit. The measured power output is approximately 100 kW and this indicates that there is something wrong with the measurements inserted into the model. Looking at the measurement of the TIT in Table 7.1, it can be seen that this value is relatively low. Turbec T100 is designed to handle a TIT of approximately 950 °C. Identifying the HMB equation in Table 4.1 regarding the isentropic efficiency of the turbine it can be seen that the low TIT results in a low  $\Delta T$  over the turbine and hence the isentropic efficiency becomes poor i.e. less than 70 %. The compressor outlet temperature is relatively high, giving a high  $\Delta T$  over the compressor. Hence, more shaft power needed to drive the compressor, as seen in Table 4.1.

The efficiency of the Turbec is calculated by:

$$\eta_{Turbec} = \frac{\text{Power output}}{(m_3 \cdot h_3) - (m_2 \cdot h_2)} \quad (7.1)$$

Because the power output in this case is negative, the electrical efficiency becomes negative, this is considered to be an unrealistic value.

Assuming the compressor outlet conditions are measured correctly and setting the power output equal to the measured value, the TIT and isentropic efficiency of the turbine can be

calculated. The input values are listed up in Table 7.3 and the results are presented in Table 7.4. This validation will be referred to as case 2.

**Table 7.3 Measurements from RGC inserted in the model**

no.	Amb. P bar	Amb. T C	Amb. Phi %	Fuel flow kg/s	COP bar	Delta P HTX bar	TIP bar	TOT C	Power output kW
1	1.007	2.5	92	0.0083871	3.8000411	0.2134798	3.4614396	615.5000000	99.50
2	1.007	2.5	92	0.0083861	3.7985556	0.2085560	3.4587796	615.4000000	99.70
3	1.0083	4.5	81	0.0083557	3.7729319	0.2128716	3.4353320	624.7000000	99.10
4	1.0083	4.5	81	0.0083555	3.7749543	0.2134985	3.4368863	624.5000000	99.11
5	1.012	4.6	83	0.0082823	3.7601003	0.2092572	3.4238825	623.1000000	98.57
6	1.012	4.6	83	0.0082792	3.7624921	0.2097367	3.4253456	624.4000000	99.23
7	1.012	5.8	67	0.0082259	3.7436743	0.2087286	3.4083090	627.5000000	100.20
8	1.012	5.8	67	0.0082238	3.7477726	0.2085884	3.4120430	627.0000000	100.11
9	1.0087	3.1	80	0.0083379	3.7614633	0.2081082	3.4247249	618.2000000	99.14
10	1.0087	3.1	80	0.0083374	3.7633970	0.2087424	3.4263818	618.4000000	100.37
11	1.0092	4.4	63	0.0083022	3.7477975	0.2076547	3.4133043	621.6000000	100.35
12	1.0092	4.4	63	0.0082996	3.7293005	0.2077706	3.3940262	621.3000000	100.18

**Table 7.4 Results from the calculation**

no.	TIT C	eta_sturb	m2 kg/s	h2 kJ/kg	m3 kg/s	h3 kJ/kg	efficiency Turbec %
1	958.02	1.0721	0.78228	580.68	0.79067	1070.4	25.37755052
2	958.25	1.0736	0.78153	580.57	0.78992	1070.7	25.43143707
3	966.75	1.0702	0.77845	590.9	0.78681	1081.1	25.36900342
4	966.68	1.0703	0.77821	590.68	0.78657	1081	25.37319362
5	964.1	1.0713	0.77408	589.12	0.78237	1077.8	25.45631442
6	966.99	1.0739	0.77029	590.57	0.77857	1081.4	25.63847948
7	973.26	1.0828	0.75877	593.73	0.76699	1088.7	26.05863186
8	972.95	1.0827	0.75829	593.17	0.76652	1088.4	26.03739359
9	958.63	1.0731	0.78188	583.4	0.79022	1070.5	25.43474858
10	961.44	1.0788	0.7764	583.62	0.78474	1074.1	25.75130424
11	965.59	1.0815	0.77098	586.88	0.77929	1078.7	25.85358166
12	963.64	1.0821	0.77417	586.55	0.78247	1076.2	25.81926818

From the results in Table 7.4 it can be seen that the isentropic efficiency of the turbine is larger than 1, which is an unattainable value. The TIT is calculated to be higher than the design limit of 950 °C. As the power output depends on the power produced by the turbine and the shaft power required by the compressor it is revealed that the assumption of correct measured compressor outlet conditions is wrong. If the isentropic efficiency of the compressor is set to a higher value, the compressor outlet temperature will decrease, and hence the shaft power needed will decrease. This will lead to a decrease in the TIT needed to produce the given power output, and result in a lower isentropic efficiency of the turbine. All

these HMB equations can be identified in Table 4.1. It has also been discovered that the compressor provides a lower pressure ratio than the one specified by Turbec. The pressure ratio in the model is calculated to approximately 3,7: 1 and the pressure ratio specified by Turbec is 4,5: 1. A higher compressor outlet pressure would increase the compressor outlet temperature for a given isentropic efficiency.

As the results from the validation did not turn out as expected it has been decided to look at the performance of the Turbec when the pressure ratio is set to 4,5 and the isentropic efficiency of the compressor set to 76 %, which is a lower limiting value for isentropic efficiency regarding a centrifugal compressor. From the measurements regarding the pressure before and after the combustion chamber, it has been discovered that the pressure drop during combustion is approximately 3,5 %. This value has been used in the model. Instead of using the TIT measured by the AC-flow system, the TIT calculated by Turbec's internal system is used in the model. The input data are listed in Table 7.5 and the results are presented in Table 7.6, and it will be referred to as case 3.

**Table 7.5 Measurements from RGC inserted in the model**

no.	Amb. P bar	Amb. T C	Amb. Phi %	Fuel flow kg/s	COP bar	Delta P HTX bar	TIP bar	TIT by Turbec C	TOT C
1	1.007	2.5	92	0.0083871	4.5315000	0.2134798	4.1668895	909.5000000	615.5
2	1.007	2.5	92	0.0083861	4.5315000	0.2085560	4.1716410	909.2000000	615.4
3	1.0083	4.5	81	0.0083557	4.5373500	0.2128716	4.1731216	922.3000000	624.7
4	1.0083	4.5	81	0.0083555	4.5373500	0.2134985	4.1725167	921.1000000	624.5
5	1.012	4.6	83	0.0082823	4.5540000	0.2092572	4.1926768	918.7000000	623.1
6	1.012	4.6	83	0.0082792	4.5540000	0.2097367	4.1922141	919.6000000	624.4
7	1.012	5.8	67	0.0082259	4.5540000	0.2087286	4.1931869	924.2000000	627.5
8	1.012	5.8	67	0.0082238	4.5540000	0.2085884	4.1933222	922.9000000	627.0
9	1.0087	3.1	80	0.0083379	4.5391500	0.2081082	4.1794553	911.9000000	618.2
10	1.0087	3.1	80	0.0083374	4.5391500	0.2087424	4.1788433	912.0000000	618.4
11	1.0092	4.4	63	0.0083022	4.5414000	0.2076547	4.1820642	916.2000000	621.6
12	1.0092	4.4	63	0.0082996	4.5414000	0.2077706	4.1819524	916.1000000	621.3

**Table 7.6 Results from the calculation**

no.	Power	eta_sturb	m2	h2	m3	h3	efficiency Turbec
	kW		kg/s	kJ/kg	kg/s	kJ/kg	%
1	83.093	0.8466	0.89643	580.68	0.90482	1008.6	21.19381586
2	82.96	0.84562	0.89688	580.57	0.90527	1008.2	21.16371922
3	84.017	0.84848	0.88143	590.9	0.88979	1024.3	21.51111038
4	83.406	0.84645	0.88408	590.68	0.89244	1022.8	21.35443662
5	81.994	0.84265	0.87926	589.12	0.88755	1019.9	21.17490077
6	81.745	0.84105	0.87968	590.57	0.88796	1020.9	21.12242538
7	81.486	0.84231	0.86993	593.71	0.87815	1026.1	21.18811238
8	80.973	0.84078	0.87188	593.15	0.8801	1024.4	21.06374512
9	82.089	0.84285	0.8918	583.38	0.90013	1011	21.06071207
10	82.03	0.84241	0.89201	583.6	0.90035	1011.1	21.04591507
11	81.607	0.84213	0.88531	586.88	0.89361	1015.7	21.02899529
12	81.698	0.84288	0.88458	586.55	0.89288	1015.6	21.05843638

The results presented in case 3 are more realistic than the results from case 1 and 2 discussed above. A power output of approximately 82 kW is achieved and the turbine has an isentropic efficiency of 84 %. If the TIT and the isentropic efficiency of the compressor were increased, a higher power output could be obtained.

The power output from the results a plotted in a graph shown in Figure 7.1 below. The numbers on the x-axis denotes the 12 groups of data that has been used for this validation.

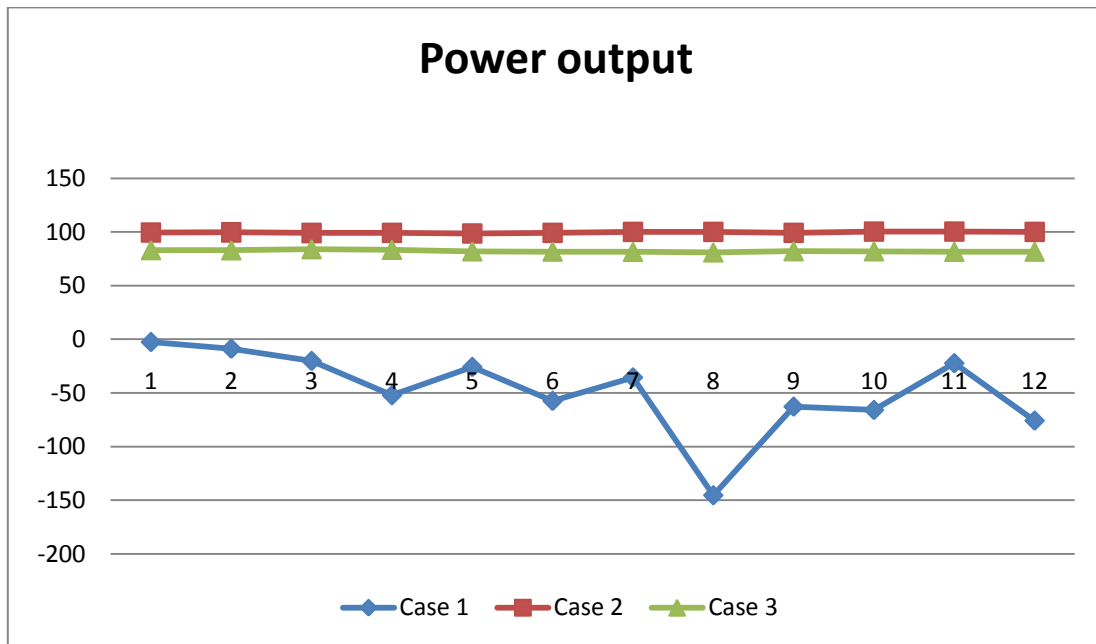


**Figure 7.1 Power output**

As it can be seen in Figure 7.1 the results of the power output from case 1 in table 7.2 are very unstable. The reason for this is the large variation in TIT, as shown in Table 7.1. The TIT should be a more stable value in order to obtain complete combustion, as described in chapter 2.4.2, thereby obtaining a stable power output. There are several reasons for the large variation of the TIT:

- There is only one probe measuring the TIT.
- TIT is a difficult value to measure, due to the dynamics of combustion.
- The cooling air leads to variation of the temperature.
- A swirl is generated at the combustion outlet causing a large variation of the temperature within a short period of time.

The power output results from case 2 shown in Table 7.3 are very stable at approximately 100 kW, as these are the power outputs measured by Turbec. The results of the power output from case 3 shown in Table 7.6 are also very stable because the TIT calculated by Turbec's internal system is more stable, the largest difference in TIT is approximately 14,5 °C.

The electrical efficiency for the results having a positive power output is plotted in the graph shown in Figure 7.2. The electrical efficiencies are calculated by equation 7.1, and is approximately 25,5 % for the results in case 2 and it is just above 21 % for the results in case 3. These are realistic values. As there is a heat exchanger utilizing hot exhaust gases to heat up water for district heating the total efficiency for the whole system is probably higher, approximately 60 %. However the validation of the district heating system including the additional heat exchanger has not been part of this work.

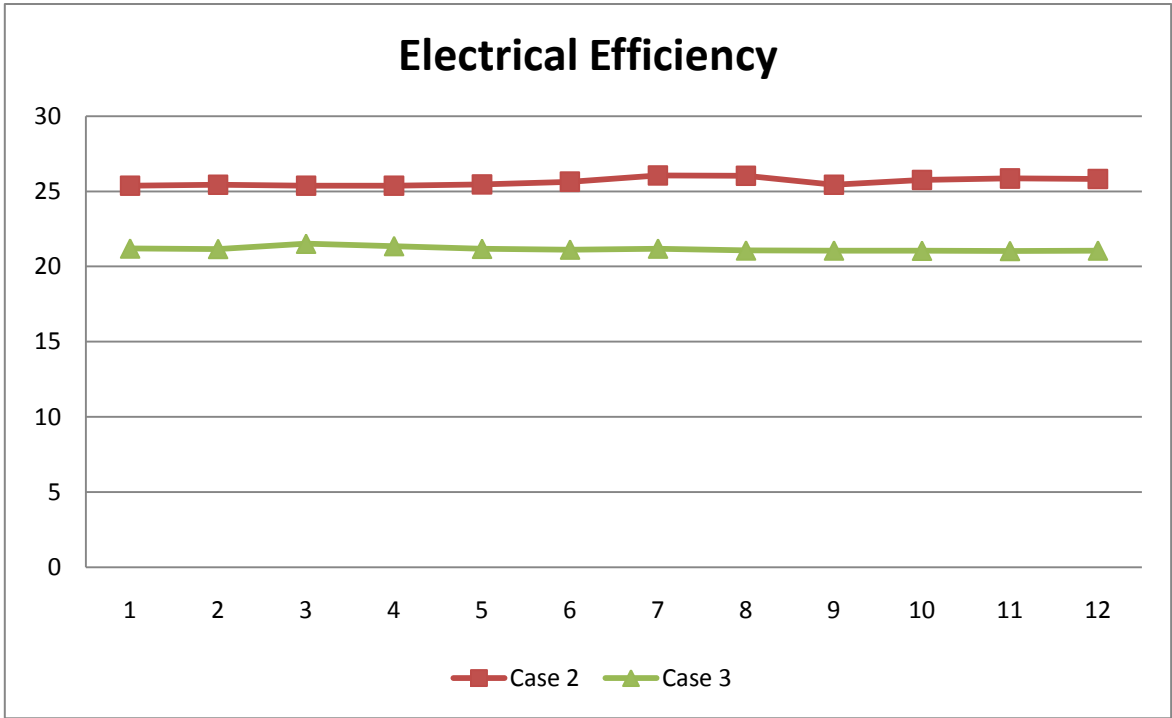


Figure 7.2 Electrical efficiency

## 8 Conclusion and Future Work

In this thesis there has been done a literature study of the theory and thermodynamics of gas turbines, microturbines and HMBP. This knowledge has been implemented in order to develop a model of the Turbec T100 stationed at RGC in the HMPB IPSEpro.

Through the literature study it has been shown that a gas turbine consist of three main components; compressor, combustion chamber and turbine. The compressor provides a pressure ratio in order to produce an expansion through the turbine. Energy is added to the system in terms of fuel that are mixed with compressed air and then ignited. The rise in temperature results in the turbine providing a useful power output in addition to driving the compressor.

The major differences between regular gas turbines and microturbines are the power produced and the size of the system. Regular gas turbines are marketed as 40 – 50 MW engines, which require a high pressure ratio. In order to achieve a high pressure ratio the gas turbine often consists of axial rotating equipment. Microturbines however, usually have a power output of 10 – 200 kW and thereby a lower pressure ratio is needed. These engines are installed with radial rotating equipment. Due to the low pressure ratio a recuperator is also installed to the system, preheating the compressed air before the combustion, resulting in a higher total efficiency.

The Turbec T100 installed at RGC has some modifications due to research purposes. The combustion chamber is installed outside the casing of the Turbec with a bypass connected to it. This bypass provides the opportunity to replace the combustion chamber with e.g. a fuel cell. There are also installed additional sensors, measuring pressure and temperature out of the compressor, after the recuperator, and at the turbine inlet. These measurements have been utilized to validate the model of the Turbec T100 at RGC created in the HMBP IPSEpro.

IPSEpro consist of three program tools: PSE, MDK and PSExcel. In PSE process models can be created by selecting components from a library and linking them together. It is also possible to modify and create new models with the MDK tool. Different input data is implemented to the components in order for PSE to solve the built in or modified equations. PSE solves the equations thermodynamically by the semi-parallel method.

PSExcel is a tool for creating variations in the model and presenting requested output data in an excel work sheet. In this thesis PSExcel has been used to create a variation of the ambient conditions to generate output data for Mats Mathisen's master thesis *Noise Filtering from a Nonlinear System by Using AANN*.

In the validation of the IPSE model it was expected that the calculated power output would be close to reality using the values from the different measurement systems at RGC. As this did not happen it was discovered that there is probably something wrong with the sensor measuring the turbine inlet temperature. This probe will now be removed from the system and calibrated before it is reinstalled into the Turbec. It is recommended, if possible, to install more measuring sensors at the combustion outlet, in order to get more accurate measurements of the turbine inlet temperature.

It has also been discovered that the pressure ratio in the compressor is much lower than the design pressure ratio of 4,5: 1. A further examination of the compressor and its behavior should be done, in order to find why it does not meet the designed standard.

The different measurement systems should be synchronized. This will make it easier to find the corresponding measurements needed to validate the HMB model. A new sample of measurements can then be taken and implemented in the model in order to make a new validation. If the IPSE model does not converge to the measured power output, an improvement of the model can be done by using the MDK tool.



## Bibliography

- [1] Yunus A. Çengel and Michael A. Boles *Thermodynamics an Engineering Approach* 5<sup>th</sup> edition
- [2] HHH Saravanamuttoo, GFC Rogers, H Cohen *Gas Turbine Theory* 5<sup>th</sup> edition
- [3] Meherwan P. Boyce *Gas Turbine Engineering Handbook* 2<sup>nd</sup> edition (pdf)
- [4] *The Jet Engine* 5<sup>th</sup> edition written by Rolls Royce (pdf)
- [5] David Japikse and Nicholas C. Baines *Introduction to Turbomachinery*
- [6] Olav Bolland *Thermal Power Generation* 2008 (pdf)
- [7] *Turbec T100 CHP system Technical description version 5.0*, Turbec AB (pdf)
- [8] Dr. N. Lymberopoulos *Microturbines and their applications in bio-energy* 2004 (pdf)
- [9] Pernilla Olausson *On the Selection of Methods and Tools for Analysis of Heat and Power Plants* Doctoral Thesis 2003
- [10] Thomas Palmé *Gas Turbine Modeling for Degradation Tracking and Monitoring with Artificial Neural Networks* Master of Science Thesis 2008
- [11] Jure Smrekar *Measuring System at RGC for GT-T100* (pdf)
- [12] *IPSEpro Process Simulator, Process Simulation Environment version 4.0.001* written by SimTech (pdf)
- [13] *IPSEpro Process Simulator, Model Development Kit version 4.0.001* written by SimTech (pdf)
- [14] *IPSEpro Process Simulator, PSExcel version 4.0.003* written by SimTech (pdf)
- [15] Björn Fredriksson Möller *A Thermo-economic Evaluation of CO<sub>2</sub> Capture with Focus on Gas Turbine Based Power Plants* Doctoral Thesis 2005

## Appendix

This appendix includes the measurements from the different measuring systems.

**Table A. 1 Measurements of the ambient conditions by the weather station installed at University of Stavanger**

Date/Time	Ambient P	Ambient T	Ambient phi
	bar	C	%
21.04.2010 08:29	1.007	2.5	92
21.04.2010 08:30	1.007	2.5	92
21.04.2010 08:31	1.007	2.5	92
21.04.2010 08:32	1.007	2.5	92
21.04.2010 08:33	1.007	2.5	92
21.04.2010 08:34	1.007	2.5	92
21.04.2010 10:33	1.0083	4.5	81
21.04.2010 10:34	1.0083	4.5	81
21.04.2010 10:35	1.0083	4.5	81
21.04.2010 10:36	1.0083	4.5	81
21.04.2010 10:38	1.0083	4.5	81
21.04.2010 10:37	1.0083	4.5	81
22.04.2010 08:30	1.012	4.6	83
22.04.2010 08:31	1.012	4.6	83
22.04.2010 08:32	1.012	4.6	83
22.04.2010 08:33	1.012	4.6	83
22.04.2010 08:34	1.012	4.6	83
22.04.2010 08:35	1.012	4.6	83
22.04.2010 10:30	1.012	5.8	67
22.04.2010 10:31	1.012	5.8	67
22.04.2010 10:32	1.012	5.8	67
22.04.2010 10:33	1.012	5.8	67
22.04.2010 10:34	1.012	5.8	67
22.04.2010 10:35	1.012	5.8	67
23.04.2010 08:27	1.0087	3.1	80
23.04.2010 08:28	1.0087	3.1	80
23.04.2010 08:29	1.0087	3.1	80
23.04.2010 08:30	1.0087	3.1	80
23.04.2010 08:31	1.0087	3.1	80
23.04.2010 08:32	1.0087	3.1	80
23.04.2010 10:27	1.0092	4.4	63
23.04.2010 10:28	1.0092	4.4	63
23.04.2010 10:29	1.0092	4.4	63
23.04.2010 10:30	1.0092	4.4	63
23.04.2010 10:31	1.0092	4.4	63

23.04.2010 10:32	1.0092	4.4	63
------------------	--------	-----	----

**Table A. 2 Measurements of the fuel flow by the SCADA system**

Date/time	Fuel flow
	Nm3/h
21.04.2010 08:29	35.95224
21.04.2010 08:30	35.95135
21.04.2010 08:31	35.94654
21.04.2010 08:32	35.94478
21.04.2010 08:33	35.94059
21.04.2010 08:34	35.93542
21.04.2010 10:33	35.81053
21.04.2010 10:34	35.81004
21.04.2010 10:35	35.81091
21.04.2010 10:36	35.80949
21.04.2010 10:38	35.80767
21.04.2010 10:37	35.80618
22.04.2010 08:30	35.49566
22.04.2010 08:31	35.49147
22.04.2010 08:32	35.48431
22.04.2010 08:33	35.48218
22.04.2010 08:34	35.47779
22.04.2010 08:35	35.47042
22.04.2010 10:30	35.25571
22.04.2010 10:31	35.25276
22.04.2010 10:32	35.25379
22.04.2010 10:33	35.24953
22.04.2010 10:34	35.24881
22.04.2010 10:35	35.24471
23.04.2010 08:27	35.74744
23.04.2010 08:28	35.74318
23.04.2010 08:29	35.73911
23.04.2010 08:30	35.73405
23.04.2010 08:31	35.73186
23.04.2010 08:32	35.72512
23.04.2010 10:27	35.58075
23.04.2010 10:28	35.57615
23.04.2010 10:29	35.56988
23.04.2010 10:30	35.56529
23.04.2010 10:31	35.56082
23.04.2010 10:32	35.56052

**Table A. 3 Measurements by Turbecs internal system**

Date/Time	Power output	TOT	TIT estimated by Turbec
	kW	C	C
21.04.2010 08:29	99.81	615.7	909.5
21.04.2010 08:30	99.22	615.4	909.5
21.04.2010 08:31	100.00	615.5	909.4
21.04.2010 08:32	99.50	615.5	909.5
21.04.2010 08:33	99.70	615.4	909.2
21.04.2010 08:34	99.94	615.4	909.5
21.04.2010 10:33	100.38	624.0	919.8
21.04.2010 10:34	99.10	624.7	922.3
21.04.2010 10:35	100.00	624.6	920.8
21.04.2010 10:36	99.11	624.5	921.1
21.04.2010 10:38	99.50	624.7	921.4
21.04.2010 10:37	99.60	626.8	924.0
22.04.2010 08:30	98.57	623.1	918.7
22.04.2010 08:31	99.30	623.0	918.6
22.04.2010 08:32	99.26	623.4	918.9
22.04.2010 08:33	99.23	624.4	919.6
22.04.2010 08:34	99.70	623.4	918.6
22.04.2010 08:35	100.44	623.5	918.6
22.04.2010 10:30	100.20	627.3	923.4
22.04.2010 10:31	100.20	626.4	922.6
22.04.2010 10:32	100.20	627.5	924.2
22.04.2010 10:33	99.40	626.8	923.1
22.04.2010 10:34	99.70	626.9	922.9
22.04.2010 10:35	100.11	627.0	922.9
23.04.2010 08:27	99.70	618.4	912.1
23.04.2010 08:28	100.10	618.5	912.4
23.04.2010 08:29	100.04	618.0	911.9
23.04.2010 08:30	99.14	618.2	911.9
23.04.2010 08:31	100.37	618.4	912.0
23.04.2010 08:32	99.80	618.5	911.5
23.04.2010 10:27	100.35	621.6	916.2
23.04.2010 10:28	100.20	621.6	916.6
23.04.2010 10:29	100.18	621.3	916.1
23.04.2010 10:30	99.50	621.6	916.2
23.04.2010 10:31	100.20	621.9	916.7
23.04.2010 10:32	99.02	621.2	915.7

**Table A. 4 Measurements by AC-flow**

Date/Time	Compressor outlet P Acflow	Compressor outlet T Acflow	P after HTX	Turbine inlet pressure	TIT Acflow
	bar	C	bar	bar	C
21.04.2010 08:29	3.796929	208.120403	3.58289877	3.457204375	788.90979760
21.04.2010 08:30	3.79899047	208.139601	3.58428697	3.45761975	799.26060190
21.04.2010 08:31	3.79841403	208.220003	3.58423342	3.458848578	813.60179900
21.04.2010 08:32	3.80004106	208.312898	3.5865613	3.461439609	822.74489400
21.04.2010 08:33	3.79855563	208.197403	3.58444552	3.458779641	817.20431320
21.04.2010 08:34	3.79952731	208.293898	3.58537044	3.460131438	827.24061010
21.04.2010 10:33	3.76746403	209.167905	3.55427984	3.429710219	803.56461040
21.04.2010 10:34	3.77293194	209.2697	3.56006031	3.435332	816.76860800
21.04.2010 10:35	3.77202784	209.413903	3.55825194	3.432879063	798.65310200
21.04.2010 10:36	3.77495425	209.566798	3.56145572	3.436886344	793.65419900
21.04.2010 10:38	3.77129553	209.612799	3.55840191	3.434505766	753.94079700
21.04.2010 10:37	3.7726155	209.694803	3.55962423	3.435329547	778.57999800
22.04.2010 08:30	3.76010025	209.4854	3.55084302	3.423882516	809.58169460
22.04.2010 08:31	3.76389559	209.497902	3.55478658	3.427871688	812.72319310
22.04.2010 08:32	3.76423947	209.3434	3.55448727	3.426792797	818.51410860
22.04.2010 08:33	3.76249206	209.418299	3.55275535	3.425345563	788.84319780
22.04.2010 08:34	3.76172528	209.487801	3.551874	3.424894281	766.87979690
22.04.2010 08:35	3.76400891	209.532299	3.55470044	3.426709453	761.86044993
22.04.2010 10:30	3.73928291	210.094299	3.53065958	3.4042125	807.86210530
22.04.2010 10:31	3.74039413	210.101697	3.5314828	3.405861734	798.57719890
22.04.2010 10:32	3.74367425	210.055501	3.53494566	3.408309047	806.46540640
22.04.2010 10:33	3.74180344	210.023203	3.53324747	3.408309047	781.33299820
22.04.2010 10:34	3.74237922	210.2671	3.53411184	3.408257531	742.76002900
22.04.2010 10:35	3.74777259	210.506301	3.53918416	3.412042969	746.20970720
23.04.2010 08:27	3.760388	208.360198	3.55228191	3.424774094	815.13671870
23.04.2010 08:28	3.75996278	208.477898	3.55198226	3.424019844	790.34249780
23.04.2010 08:29	3.76016775	208.608398	3.55214642	3.424250203	786.35930060
23.04.2010 08:30	3.76146334	208.640201	3.55335513	3.424724922	779.33080190
23.04.2010 08:31	3.763397	208.717101	3.55465458	3.426381844	777.71595902
23.04.2010 08:32	3.76334234	208.681102	3.55514387	3.426622234	756.85686581
23.04.2010 10:27	3.74779754	209.9529	3.5401428	3.413304344	810.75213210
23.04.2010 10:28	3.74613628	209.925604	3.53727588	3.409410344	774.40650460
23.04.2010 10:29	3.72930047	209.6417	3.52152986	3.394026188	773.84989730
23.04.2010 10:30	3.71187359	209.0921	3.5049861	3.378073016	768.95289890
23.04.2010 10:31	3.70305341	208.676102	3.49706164	3.37022725	758.12769410
23.04.2010 10:32	3.71862503	208.9871	3.51159916	3.384488344	724.80060570